

# **Characterization of Cu<sub>2</sub>O-ZnO Interface for Photosensitive Devices**

**by**

**Muyar Htun**

B.E., Yangon Technological University, 2006

Project Submitted in Partial Fulfillment of the  
Requirements for the Degree of  
Master of Engineering

in the

School of Engineering Science  
Faculty of Applied Sciences

**© Muyar Htun 2015**

**SIMON FRASER UNIVERSITY**

**Summer 2015**

All rights reserved.

However, in accordance with the *Copyright Act of Canada*, this work may be reproduced, without authorization, under the conditions for "Fair Dealing." Therefore, limited reproduction of this work for the purposes of private study, research, criticism, review and news reporting is likely to be in accordance with the law, particularly if cited appropriately.



## Abstract

This project investigates the photo sensitive characteristics of  $\text{Cu}_2\text{O}$ -ZnO interface from painted cuprous oxide on copper. Existing methods of producing  $\text{Cu}_2\text{O}$ -ZnO photosensitive layers are complex, costly and require high temperature conditions. The paintable medium developed in our approach was a simple mixture of cuprous chloride, adhered hydrate cuprous oxide, de-ionised water and acetone. The prepared medium was painted on a clean copper sheet. The device was then heated at  $75^\circ\text{C}$  for 30 minutes. The ZnO layer was electroplated in zinc nitrate solution at  $72^\circ\text{C}$ . The surfaces of  $\text{Cu}_2\text{O}$  and ZnO were analyzed by SEM and the results showed homogenous surface morphology. The photosensitivity of the manufactured  $\text{Cu}_2\text{O}$ -ZnO was also characterized using a semiconductor parameter analyser (SPA) and a light source. The manufactured devices exhibited ohmic (I-V) characteristics in the dark. Upon illumination, the current density increased by 40 %. Samples that were annealed for two-hours at  $75^\circ\text{C}$  before ZnO electrodeposition, exhibited a solar-cell type (I-V) response.

**Keywords:**  $\text{Cu}_2\text{O}$ -ZnO; photosensitivity; paintable medium; homogenous surface morphology; solar cell type (I-V) behavior

## **Dedication**

To my supervisor Dr. Ash Parameswaran, my beloved family and raped victims who are struggling to get their normal lives back.

## **Acknowledgements**

First of all I'm deeply thankful to my supervisor, Dr. Ash Parameswaran, for his guidance, support, patience and giving me a second chance. Working under him was a very pleasant experience and I was able to gain a lot of knowledge and experience. Without his support, this research would never have been completed.

I would like to thank to Dr. Mahendra Prasad for sharing me his time to helping me finish my project and guiding me through every step of my work.

Sincere thanks to Dr. Andrew Rawicz for agreeing to be the examiner for my project presentation.

I would like to thank to associate dean of graduate studies, Dr. Mary-Ellen Kelm, for helping me in pursuing my dream. I would also like to thank to Dr. Mitchell Stoddard - director, Centre for Students with Disabilities.

Special thanks to Shruti and Sae-Won for all the help and support they have provided.

# Table of Contents

Approval.....	ii
Abstract.....	iii
Dedication.....	iv
Acknowledgements.....	v
Table of Contents.....	vi
List of Tables.....	viii
List of Figures.....	ix
List of Acronyms.....	x

<b>Chapter 1. Introduction .....</b>	<b>1</b>
1.1. Cuprous Oxide (Cu <sub>2</sub> O) and Zinc Oxide (ZnO) Semiconductors .....	1
1.2. Motivation.....	2
1.3. Thesis Organization.....	2

<b>Chapter 2. Photosensitive devices and photosensitive materials .....</b>	<b>4</b>
2.1. Photosensitive devices .....	4
2.1.1. Photo-resistor or light dependent resistor (LDR) .....	4
2.1.2. Photodiode and solar cell .....	5
2.2. Photosensitive semiconductor materials.....	7
2.2.1. Silicon as photosensitive material.....	8
2.3. Common oxide photosensitive materials.....	8
2.3.1. Cadmium oxide (CdO).....	9
2.3.2. Nickel oxide (NiO).....	9
2.3.3. Titanium dioxide (TiO <sub>2</sub> ).....	10

<b>Chapter 3. Copper oxides and Zinc Oxide as economical photosensitive hetero-junction .....</b>	<b>11</b>
3.1. Copper Oxides.....	11
3.1.1. Cuprous oxide (Cu <sub>2</sub> O).....	11
3.1.2. Properties of Cu <sub>2</sub> O.....	12
3.1.3. Cu <sub>2</sub> O in semiconductor history .....	12
3.1.4. Various methods of preparing Cu <sub>2</sub> O.....	14
3.2. Zinc Oxide (ZnO).....	15
3.2.1. Crystal Structure of ZnO.....	15
3.2.2. Properties of ZnO.....	17
3.2.3. ZnO in semiconductor history .....	17
3.2.4. Various methods of depositing ZnO.....	17
3.3. Cu <sub>2</sub> O - ZnO Hetero-junction .....	18
3.3.1. Efficiency of Cu <sub>2</sub> O-ZnO produced by existing methods .....	19

<b>Chapter 4. Processing technique for paintable photosensitive devices .....</b>	<b>21</b>
4.1. Cu <sub>2</sub> O process technology.....	21

4.1.1.	Preparation of colloidal suspension paint for Cu <sub>2</sub> O.....	21
4.1.2.	Painting process .....	22
4.2.	ZnO deposition .....	23
4.2.1.	Electrochemical deposition .....	23
4.2.1.1.	Electrode potentials during electrochemical deposition.....	24
4.2.1.2.	Faraday's Law.....	25
4.2.1.3.	Electrochemical deposition of ZnO .....	26
4.2.1.4.	Results .....	27
4.3.	Contact electrode .....	28
4.4.	Surface Morphology .....	30
4.5.	Electrical Characteristics .....	31
4.5.1.	Hall voltage measurement for Cuprous Oxide .....	33
4.5.2.	Hall voltage measurement for Zinc Oxide .....	36
<b>Chapter 5.</b>	<b>Photosensitivity of Cu<sub>2</sub>O-ZnO device .....</b>	<b>37</b>
5.1.	Experiment and result of Cu <sub>2</sub> O-ZnO device (1) (biased voltage mV) .....	37
5.2.	Experiment and result of Cu-Cu <sub>2</sub> O-ZnO device (1) (biased voltage μV) .....	38
5.3.	Experiment and results of Cu-Cu <sub>2</sub> O-ZnO Device (2) .....	39
<b>Chapter 6.</b>	<b>Conclusion.....</b>	<b>41</b>
<b>Chapter 7.</b>	<b>Future work.....</b>	<b>43</b>
<b>References</b>	<b>.....</b>	<b>44</b>

## List of Tables

Table 3.1.	Basic properties of $\text{Cu}_2\text{O}$ [39].....	12
Table 3.2.	Fundamental properties of $\text{ZnO}$ [64].....	17
Table 4.1.	Hall Voltage measurement of cuprous oxide .....	35
Table 4.2.	Hall Voltage measurement of zinc oxide .....	36



## List of Figures

Figure 2.1.	V-I Characteristics of a photodiode .....	5
Figure 2.3.	V-I characteristics of solar cell.....	6
Figure 3.1.	Crystal structure of $\text{Cu}_2\text{O}$ [40] .....	12
Figure 3.2.	Wurzite structure of $\text{ZnO}$ [66] .....	16
Figure 3.3.	Band-structure of $\text{Cu}_2\text{O}$ - $\text{ZnO}$ hetero-junction .....	19
Figure 4.1.	Photograph of the $\text{Cu}_2\text{O}$ painted on bare $\text{Cu}$ sample .....	23
Figure 4.2.	Detail set up of $\text{ZnO}$ electrochemical deposition.....	26
Figure 4.3.	$\text{Cu}$ - $\text{Cu}_2\text{O}$ - $\text{ZnO}$ device processing steps .....	29
Figure 4.4.	A complete $\text{Cu}$ - $\text{Cu}_2\text{O}$ - $\text{ZnO}$ device with nickel painted electrodes .....	29
Figure 4.5.	(a) SEM image of $\text{Cu}_2\text{O}$ in $18\mu\text{m}$ , (b) SEM image of $\text{ZnO}$ in $20\mu\text{m}$ and (c) SEM image of $\text{ZnO}$ in $12\mu\text{m}$ .....	31
Figure 4.6.	Electrode location details. I – Current electrodes and V – Hall voltage probing electrodes .....	34
Figure 4.7.	Voltage discharge through copper.....	35
Figure 5.1.	V-I response of the $\text{Cu}$ - $\text{Cu}_2\text{O}$ - $\text{ZnO}$ device (biased voltage $\text{mV}$ range) .....	38
Figure 5.2.	V-I response of the $\text{Cu}$ - $\text{Cu}_2\text{O}$ - $\text{ZnO}$ device (biased voltage $\mu\text{V}$ range) .....	39
Figure 5.3.	V-I response of the device observed as a solar cell.....	40

## List of Acronyms

CAD	Chemical vapor deposition
CdTe	Cadmium telluride
CdO	Cadmium oxide
Cu <sub>2</sub> O	Cuprous oxide
DC	Direct current
FF	Fill factor
GaAs	Gallium arsenide
KOH	Potassium hydroxide
LDR	Light dependant resistor
LiOH	Lithium hydroxide
M-MOS	Metal metal-oxide semiconductor
NaOH	Sodium hydroxide
NiO	Nickel oxide
PbS	Lead sulfide
PbSe	Lead selenide
RF	Radio frequency
SEM	Scanning electron microscope
TEM	Transmission electron microscopy
TiO <sub>2</sub>	Titanium dioxide
XPS	X-ray photoelectron spectroscopy
ZnO	Zinc oxide

# Chapter 1.

## Introduction

### 1.1. Cuprous Oxide (Cu<sub>2</sub>O) and Zinc Oxide (ZnO) Semiconductors

Metal Metal-oxide interfaces (M-MOS) take part a major role in electronic and optical applications. Due to their electrical properties, the M-MOS can be used as insulators, conductors and superconductors [1]. Moreover, they can also be used as optical and photo sensitive devices such as light emitting diodes, photoconductors and solar cells [1, 2]. Cu<sub>2</sub>O and ZnO are the most popular among the various types of M-MOS since they are non-toxic, abundant, inexpensive and simple to produce. Furthermore, they have a relatively high light absorption coefficient [3]. Common techniques used to develop Cu<sub>2</sub>O include thermal oxidation, electrochemical deposition, sol-gel spray and sputtering. Existing techniques used to develop Cu<sub>2</sub>O require complicated procedures and some require high temperature conditions of at least 200° Celsius [4]. Therefore, we have investigated a simple and unique painting method to develop Cu<sub>2</sub>O on the surface of copper. This painting method does not require a complicated instrumental set up and can be performed at a far lower temperature than those required in existing methods [4].

A hetero-junction is an active interface for many semiconductor devices [5]. Typically a hetero-junction will comprise of n-type and p-type semiconductor with different bandgaps [5]. An n-type semiconductor is one which has a majority of electron carriers and a p-type semiconductor is one which has a majority of holes. Thus, an n-type semiconductor, zinc oxide (ZnO), and p-type semiconductor, Cu<sub>2</sub>O were used to achieve the hetero-junction and this combination of hetero-junction has been the most notably investigated semiconductor [6-8]. The most commonly used method to produce

Cu<sub>2</sub>O-ZnO is electrochemical deposition of both materials [6-8]. While Cu<sub>2</sub>O has typically been created using electrochemical deposition, however research has been done investigating sputtering and annealing of ZnO instead of electrochemical deposition [9,10].

Although in the past research has been conducted on the electrical properties of Cu<sub>2</sub>O and ZnO, nowadays most research primarily focuses on the photosensitive properties of Cu<sub>2</sub>O and ZnO, which proves to be useful for photo-detectors, photodiodes and solar cell applications [10-12].

## **1.2. Motivation**

Cu<sub>2</sub>O is one of the most attractive materials for various applications such as photo-sensitive and photovoltaic applications. Moreover, literature reports a theoretical energy conversion efficiency of Cu<sub>2</sub>O is approximately 20%, while the maximum energy conversion efficiency that was observed was only a 3.8% [13, 14]. There are various preparation techniques to develop Cu<sub>2</sub>O: thermal oxidation, electrochemical deposition, sputtering, anodic oxidation and sol-gel chemistry methods. However, no prior research has been done on developing M-MOS photosensitive Cu<sub>2</sub>O devices by a simple painting method. Therefore, this research explored a simple and unique process of depositing Cu<sub>2</sub>O by painting a colloidal solution mixture of cuprous-cupric chloride on cleaned copper sheet. The painting method provided a homogenous Cu<sub>2</sub>O layer on top of copper sheet and that allowed the investigation of its photosensitivity. The painting technique is economical, simple and can also be performed under lower temperature conditions which are attractive for low cost manufacturing process.

## **1.3. Thesis Organization**

Chapter 2 presents photosensitive materials and their role as semiconductors.

Chapter 3 presents copper oxide and ZnO as economical photosensitive materials and a literature review on existing methods of producing both materials.

Chapter 4 presents device processing technique of Cu-Cu<sub>2</sub>O-ZnO device.

Chapter 5 presents photo-sensitivity of the device.

Chapter 6 and Chapter 7 present conclusion and future work.

## **Chapter 2.**

# **Photosensitive devices and photosensitive materials**

## **2.1. Photosensitive devices**

Photosensitive devices are used to convert optical energy into electrical energy. There are several types of photosensitive devices such as photo-resistors, photodiodes and solar cells.

### **2.1.1. Photo-resistor or light dependent resistor (LDR)**

A photo resistor is a semiconductor device whose resistance alters when it is illuminated by light source. Depending on the materials used for photoresistor production, there are two types of photoresistors: intrinsic and extrinsic. In an intrinsic photoresistor, light stimulates the electrons from the valance band and makes those electrons jump to the conduction band. As a result, there are more free electrons present in the device to increase current flow and decrease the resistance of the device. Extrinsic photoresistors can be produced by doping impurities to the semiconductor material. In this way a new band is generated above the valance band. The electrons from the new band need lesser energy to transfer to the conduction band and when the surface is illuminated, the electrons movement increases, and thus allows current flow [15].

During the 1930s, silicon, germanium and selenium were used to produce photoresistors. Nowadays most commercial photoresistors are made from cadmium sulfate which is highly toxic and banned in many countries [16]. Therefore, in those countries, alternative devices such as photodiodes have to be used instead of

photoresistors. Therefore, there is a commercial need for photoresistors manufactured from non-toxic and low cost materials.

### 2.1.2. Photodiode and solar cell

The exposure of light generates electron-hole pairs in a photodiode and those carriers contribute to the photosensitivity of the material. A photodiode can be p-n photodiode or p-i-n photodiode [17]. Semiconductor materials such as  $\text{Cu}_2\text{O}$ ,  $\text{ZnO}$ , Silicon(Si), gallium arsenide (GaAs), lead selenide (PbSe) and lead sulfide (PbS) are used for photodiodes [17,18]. Photodiodes are used in blood spectrum analysers, X-ray detection for CAT scanners, smoke detectors and various biomedical, safety and communication applications. Figure 2 shows V-I characteristics of a typical photodiode [18].

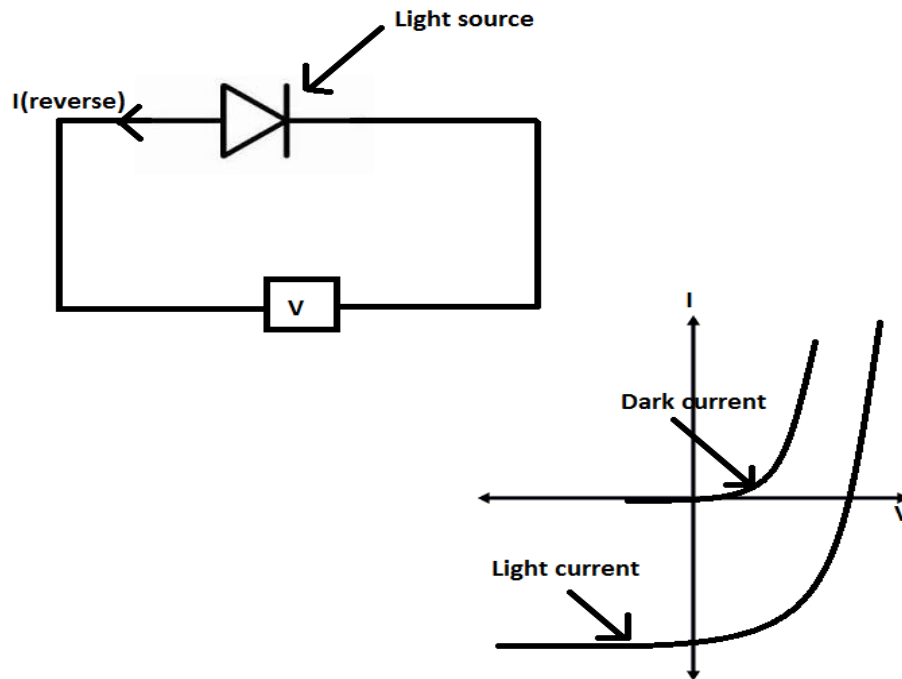


**Figure 2.1. V-I Characteristics of a photodiode**

Note: Adapted from [18]

Although the basic principles of photodiodes and solar cells are almost the same, photodiodes require a faster response time and are designed to detect light. On the

other hand solar cells are designed to generate more electrical carriers than photodiodes and also have higher energy conversion efficiency.

The standard V-I characteristics of a solar cell is shown in Figure 2.2 .There are important parameters that can be derived from the V-I characteristics such as the open circuit voltage ( $V_{oc}$ ), short circuit current ( $I_{sc}$ ), fill factor (FF) and the conversion efficiency ( $\eta$ ).  $I_{sc}$  is current through the solar cell when the voltage across the solar cell is zero and  $V_{oc}$  is voltage through the solar cell when the current is zero. Moreover,  $V_{oc}$  is maximum voltage achieved by the solar cell. Fill factor and  $\eta$  in following equations 2 and 3 describe the performance characteristics of the solar cell [19].

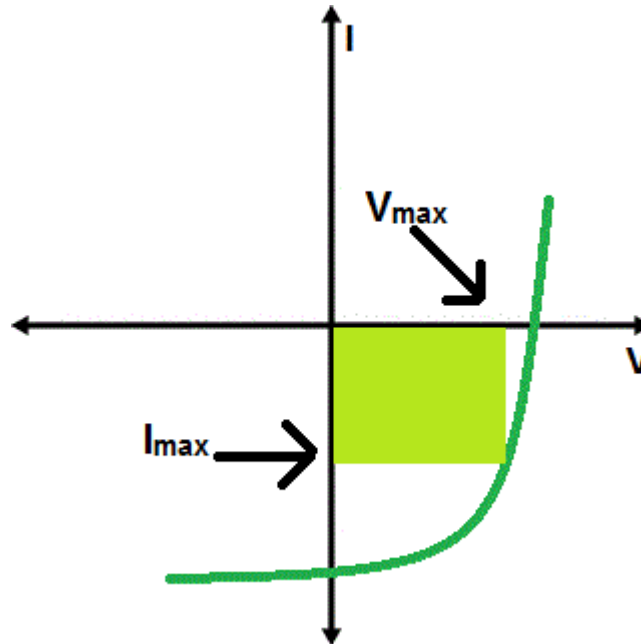


**Figure 2.2. V-I characteristics of solar cell**

The maximum power can be calculated from the values of voltage and current ( $V_{max}$  and  $I_{max}$ ) and the maximum power point is also known as the optimal working point. Therefore,

$$P_{max} = V_{max} \times I_{max} \dots\dots\dots(1)$$

The fill factor can be expressed as the ratio of the  $P_{max}$  divided by the product of  $V_{oc}$  and  $I_{sc}$  as given in Equation 2.



$$FF = \frac{P_{\max}}{V_{oc} I_{sc}}$$

(or)

$$FF = \frac{V_{oc} - \ln(V_{oc} + 0.72)}{V_{oc} + 1} \dots\dots\dots (2)$$

The conversion efficiency  $\eta$  can be calculated from power of input light provided from external light source  $P_{in}$ ,  $V_{oc}$ ,  $I_{sc}$  and FF

$$\eta = \frac{V_{oc} I_{sc} FF}{P_{in}} \dots\dots\dots (3)$$

## 2.2. Photosensitive semiconductor materials

Photosensitivity or photoconductivity of a material explains that when sufficient energy of light is exposed to the surface of certain material, the electrical conductivity of the materials increases. There are two groups of photosensitive materials: organic (polymer) and inorganic, for example, Metal Metal-Oxide (M-MOS) materials.

Organic photosensitive materials are manufactured from conductive organic polymers or small organic molecules [20]. Research on organic photosensitive materials has been going on for more than 3 decades. These materials are flexible, light weight and low-cost to manufacture although their maximum efficiency is approximately 10% which is quite low compared to the 20% theoretical energy efficiency value of  $Cu_2O$  [13,21] . There are two methods used to prepare organic photosensitive materials: thermal evaporation method and wet processing method. In the thermal evaporation method, a polymer film is deposited on the substrate within a vacuum chamber which helps remove contaminants such as water and oxygen [20]. There are four categories of wet processing methods and they are spin coating, doctor blading, screen printing and ink printing [20]. Common to all these methods is that organic materials are dissolved in an appropriate solvent such as water or any other polar or non-polar organic solvent

before forming an insoluble film on the substrate [20]. The main disadvantage of organic photosensitive materials is that polymers and organic photosensitive materials can degrade when exposed to light and the stability of real life application is still questionable although there have been tremendous efforts to reduce degradation as well as to increase life time of the materials [21].

Inorganic photosensitive materials are metalloids or M-MOS materials such as  $\text{Cu}_2\text{O}$ , cadmium telluride (CdTe), nickel oxide (NiO), Titanium oxide ( $\text{TiO}_2$ ), ZnO and amorphous silicon (a:Si) [21,22]. Most of the materials in these groups provide high efficiency and stability of the photosensitive device. A wide variety of preparation methods such as thermal oxidation, sputtering, chemical vapour deposition and electrochemical deposition are used to develop metalloids or M-MOS depending on the required materials.

### **2.2.1. Silicon as photosensitive material**

There are three types of silicon solar cells: mono-crystalline silicon (c:Si), polycrystalline silicon (p:Si) and amorphous silicon (a:Si). The very first silicon solar cell was introduced by Bell Laboratories in 1941. In 1954 silicon solar cells which provided 6% energy conversion efficiency was developed and used in satellites. Nowadays, the efficiency of silicon solar cells has reached 23%. Although silicon solar cells provide high energy conversion efficiency, there are several disadvantages. The developing process of c:Si is complex and needs to be done at high temperature conditions. The fabrication process of a:Si costs more than c:Si Therefore, oxide-based photosensitive materials are becoming popular in photovoltaic research [24].

### **2.3. Common oxide photosensitive materials**

Some M-MOS play a major role in photosensitivity and photovoltaic research due to their sensitivity to light. Many M-MOS are easy to produce, low cost, abundant, chemically stable and environmental friendly. Although commercial success has been demonstrated, their popularity is growing and based on the research being done at

present, it is clear that the future of M-MOS holds great promise. M-MOS can be used as photodiodes, photo-resistors, photo-sensors and solar cells [25 - 27].

Oxide semiconductors such as cadmium oxide (CdO), nickel oxide (NiO), Titanium oxide (TiO<sub>2</sub>), Cu<sub>2</sub>O and ZnO provide photosensitivity. They have been investigated as photodiodes, photo-resistors, photo-sensors and solar cells. While TiO<sub>2</sub> and ZnO work as transporting electrons, NiO provides hole transportation [22]. The following sub sections discuss the photosensitive properties of CdO, NiO and TiO<sub>2</sub>. Cu<sub>2</sub>O and ZnO will be discussed in greater depth in chapter 3.

### **2.3.1. Cadmium oxide (CdO)**

CdO is an n-type semiconductor that has a band gap energy between 2.2 to 2.5 eV. Due to this narrow band gap, CdO is not as attractive as other M-MOS [28]. There are several methods used to prepare CdO including, mechano-chemical, hydrothermal, solvo-thermal, chemical precipitation and micro-emulsion methods. Literature reports mechanochemical method is the most efficient, convenient as well as cost effective for CdO. CdO can be used in solar cells, gas sensors, photocatalysis, photodiodes and transparent electrodes [29]. Although CdO as a photosensitive material provides higher efficiency among oxide semiconductors, it is highly carcinogenic and toxic [30]. Therefore, cadmium oxide is not a favorable photosensitive material for commercial use.

### **2.3.2. Nickel oxide (NiO)**

NiO is a p-type semiconductor as well as a non-stoichiometric semiconductor with a wide band gap from 3.6 to 4.0 eV. It is also an anti-ferromagnetic material. The preparation methods of NiO include electron beam evaporation, vacuum evaporation, anodic oxidation, chemical deposition, rf-magnetron sputtering, sol-gel, spray pyrolysis technique and atomic layer epitaxy [31]. NiO can be used in solar thermal absorbers, photocatalysts, electrochromic devices and positive electrodes in batteries [32]. NiO has been used for hole transport as well as to enhance the charged carrier in organic solar cells [33]. Although it doesn't provide reasonable efficiency as a solar cell, it enhances the efficiency and conductivity of organic solar cells. The nature of NiO allows it to be

used as hole transport materials in organic polymer solar cells. However, NiO by itself is not an efficient photosensitive device [22].

### **2.3.3. Titanium dioxide (TiO<sub>2</sub>)**

TiO<sub>2</sub> is an n-type semiconductor and it can be prepared using chemical vapor deposition (CVD), sol-gel, electrochemical deposition, sputtering and plasma vapor deposition (PVD) techniques [34, 35]. Due to its light absorption properties, it can be used in solar cells, solar hydrogen production, solar water purification, photo-oxidation in organic pollutants and photo-killing of bacteria such as E-Coli [36].

TiO<sub>2</sub> is mostly used as an electron conductor in organic solar cells which provides an energy conversion efficiency of approximately 12%. Although TiO<sub>2</sub> layered with organic solar cells provides high efficiency, the hetero-junction layers of Cu<sub>2</sub>O/TiO<sub>2</sub> provide an energy conversion efficiency of only 0.1-1% [22].

## Chapter 3.

# Copper oxides and Zinc Oxide as economical photosensitive hetero-junction

### 3.1. Copper Oxides

Copper oxides are attractive among semiconductor materials because they are abundant, non-toxic and their preparation cost is inexpensive as well as simple. They also have favorable band-gaps and are physically and chemically stable. There are two stable types of copper oxides: cupric (CuO) and cuprous (Cu<sub>2</sub>O).

The band gap of Cu<sub>2</sub>O is approximately 2 eV and the color is reddish brown. CuO has black or dark gray color with band gap of 1.4 eV. The main property difference between Cu<sub>2</sub>O and CuO is the copper valences. Copper valences for Cu<sub>2</sub>O is Cu<sup>+</sup> and CuO is Cu<sup>2+</sup> and Cu<sub>2</sub>O is more promising material than CuO due to its high absorption coefficient. [37].

#### 3.1.1. Cuprous oxide (Cu<sub>2</sub>O)

Cu<sub>2</sub>O is a p-type semiconductor material which results from the cation deficiencies mainly caused by copper vacancies rather than oxygen interstitials or any other defects [38]. Figure 3.1 shows a simple cubic structure of Cu<sub>2</sub>O with a lattice parameter 4.2696 Å. A unit Cu<sub>2</sub>O cell has four copper atoms and two oxygen atoms with each oxygen at the centre surrounded by a tetrahedron of copper atoms [39].

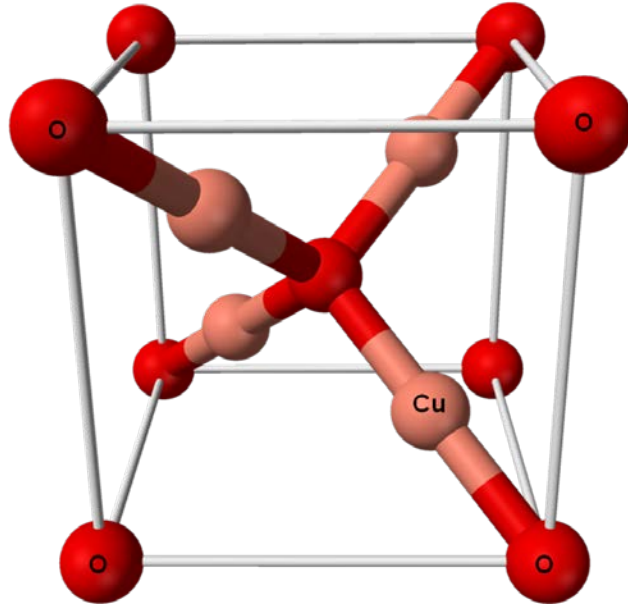


**Figure 3.1. Crystal structure of Cu<sub>2</sub>O [40]**

### 3.1.2. Properties of Cu<sub>2</sub>O

**Table 3.1. Basic properties of Cu<sub>2</sub>O [39]**

Formula weight	143.14g
Density	5.749-6.140 g/cm <sup>3</sup>
Melting point	1235 °C
Lattice constant	4.2696 Å
Thermal expansion coefficient	$2.3 \times 10^{-7} \text{ K}^{-1}(283\text{K})$
Dielectric constant	$\epsilon(0)=7.11 ; \epsilon(\infty)=6.46$
Hole hall mobility	$\mu=70 \text{ cm}^2/\text{V sec}$

### 3.1.3. Cu<sub>2</sub>O in semiconductor history

The very first Cu<sub>2</sub>O device was a rectifier invented by Grondhal in the 1920s which established the future of Cu<sub>2</sub>O in the semiconductor industry [41]. Since then, there has been a significant amount of research conducted on Cu<sub>2</sub>O rectifier characterization. By the 1940s, Cu<sub>2</sub>O rectifier research was one of the main semiconductor researches at Bell Telephone Laboratory [42]. Almost at the same time,

new semiconductor materials such as silicon and germanium became more prominent and the interest turned to these new materials.

The history of  $\text{Cu}_2\text{O}$  solar cells dates back between 1920 and 1933 although the very first solar cell was made by Charles Fritts in 1883 from selenium and gold [43]. It was reported that A.E. Becquerel discovered the photovoltaic effect in 1839 [44]. In 1888, a Russian scientist A.G. Stoletov made a solar cell which was better than the solar cell developed by Charles Fritts [45]. The fabrication of cuprous solar cells was initiated in 1930s. It was prepared by thermal oxidation on copper sheets to demonstrate the  $\text{Cu}/\text{Cu}_2\text{O}$  photovoltaic cell [46]. In 1935, E.D Wilson et al. made use of transparent  $\text{Cu}_2\text{O}$  to fabricate a photo-sensitive material [47]. However the device was limited to the visible spectrum of light of 700 to 800 nm. The real progress in solar cells fabrication was accomplished in 1940s. In 1954, Bell Laboratory successfully launched a silicon p-n junction solar cell with 6% efficiency [48]. Since then the era of solar cells began with different photosensitive materials in the world. Although the history of  $\text{Cu}_2\text{O}$  solar cells is quite primitive, research and development on  $\text{Cu}_2\text{O}$  solar cells was eventually stopped due to its low photovoltaic energy conversion efficiency (<1%). Simultaneously there had been a tremendous progress of silicon technology of photovoltaic cells which provided a higher conversion efficiency of approximately 23% [24]. However, realising the cost factor abundance of copper and easier methods of preparation of  $\text{Cu}_2\text{O}$ , researchers were encouraged to explore the application of  $\text{Cu}_2\text{O}$  for harvesting solar energy for mass consumption in different parts of the world.

Furthermore, a comprehensive review was done on  $\text{Cu}_2\text{O}$  solar cells by Nelson et.al., which emphasized the issues that need to be addressed in increasing the photovoltaic energy conversion efficiency of  $\text{Cu}_2\text{O}$  in order to make it feasible for commercial production of  $\text{Cu}_2\text{O}$  [49].

In order to get a deeper insight into these issues, fabrication and characterisation of  $\text{Cu}_2\text{O}$  solar cells was initiated under a research program during the late 1970s. This research addressed the three main areas that needed to be addressed in using  $\text{Cu}_2\text{O}$  which were: (1) complex preparation method of  $\text{Cu}_2\text{O}$  (2) increasing the photoconductivity of the materials (3) improving the p-n junction [50]. The theoretical

efficiency of  $\text{Cu}_2\text{O}$  solar cells is approximately 20% under solar illumination of AM1.5 (radiation power  $100 \text{ mW/cm}^2$ ). Rakhshani et. al., reviewed the existing methods of preparation of  $\text{Cu}_2\text{O}$  for the fabrication of the  $\text{Cu}_2\text{O}$  solar cell. This research investigated preparation methods which needed temperatures less than  $300^\circ\text{C}$  as most preparation techniques required high temperature oxidation of copper of more than  $1000^\circ\text{C}$  [51]. Since then, there has been a great deal of research on low temperature preparation of  $\text{Cu}_2\text{O}$  [52].

#### **3.1.4. Various methods of preparing $\text{Cu}_2\text{O}$**

There are many existing methods used to prepare  $\text{Cu}_2\text{O}$  such as electro-deposition, chemical vapour deposition, sputtering, anodic oxidation and sol-gel chemistry. However, the most commonly used method is thermal oxidation. Thermal oxidation is one of the simplest methods to produce  $\text{Cu}_2\text{O}$  and the thinness of the  $\text{Cu}_2\text{O}$  film can easily be adjusted by the length of the thermal oxidation time. Oxidation can be performed under the temperatures between  $200^\circ\text{C}$  to  $1500^\circ\text{C}$  and the oxidation time can vary from several hours to a couple days in order to achieve the desired thickness [4,51,53]. Moreover, thermal oxidation can be done not only in air but also water vapor and oxygen. During thermal oxidation  $\text{CuO}$  and  $\text{Cu}_2\text{O}$  can be formed depending on the thermal stability of the oxides [53]. In this method thermal stability is important if the desired copper oxide is  $\text{Cu}_2\text{O}$ . There are very few p-type semiconductors which can be electrochemically deposited and  $\text{Cu}_2\text{O}$  is one of them [54]. The quality and efficiency of  $\text{Cu}_2\text{O}$  depends on the type of aqueous solution and their pH level, deposition potential and temperature. Although n-type  $\text{Cu}_2\text{O}$  electrodeposition has been done, both p-type and n-type depositions result in low efficiency owing to the high resistivity. Doping is required in order to reduce this resistivity [55].

CVD is another method which provides high- purity and high-quality materials.  $\text{Cu}_2\text{O}$  produced by CVD can be polycrystalline or amorphous based on the materials and reactors used for the process. There are many factors that determine the quality of the deposited  $\text{Cu}_2\text{O}$  such as, the type of precursor, process temperature and pressure, gas flow rate and the design of the reactor used during CVD [55, 56].



Sputtering is a technique of emitting materials from a source to deposit on a desired substrate.  $\text{Cu}_2\text{O}$  can be deposited by using the sputtering method which needs a low pressure vacuum system. Depending on RF power and oxygen flow,  $\text{Cu}_2\text{O}$  and  $\text{CuO}$  rich deposited substrates can be produced. Moreover, the resistivity of the oxide depends on the RF power and oxygen flow. The lowest resistance of the  $\text{Cu}_2\text{O}$  substrate produced by sputtering is 10 Ohms [58, 59].

Anodic oxidation is a high speed electrochemical oxidation method which can provide natural oxide films on the metal. Anodic oxidation can produce  $\text{Cu}_2\text{O}$  on the copper surface although the purity of the  $\text{Cu}_2\text{O}$  produced by this method is still questionable. In this process, the oxide film is composed of two layers: the inner layer is  $\text{Cu}_2\text{O}$  with partly hydrated  $\text{CuO}$  and the outer layer is  $\text{CuO}_x(\text{OH})_{2-2x}$  [60, 61].

The sol-gel method is chemical transformation of liquid into gel state with post treatment and changing into solid state oxide materials. It is simple, low cost and it does not need a sophisticated work place. Moreover, its crystallization and distribution can be controlled by molecular precursors and annealing conditions used during the process. [62,63].

## **3.2. Zinc Oxide (ZnO)**

ZnO is a semiconductor which belongs to II-VI semiconductor group. ZnO can be found in a mineral called zincite which is red or manganese in colour. Zincite can also be synthetically produced. Therefore it is low cost, nontoxic and abundant. Artificial ZnO is always an n-type semiconductor with a wide band-gap energy of 3.3 eV. Therefore ZnO is a popular semiconductor material and is widely used in photovoltaic applications [64].

### **3.2.1. Crystal Structure of ZnO**

The crystalline structure of ZnO has three phases: wurtzite (hexagonal), zinc-blende (cubic) and rocksalt (cubic). The ZnO hexagonal unit cell has two molecules and the oxygen atoms surround the ZnO atoms in a tetrahedral structure [64]. In a cubic structure substrate zinc-blende can be made and rocksalt can be formed at high

pressures of 9.8 GPa at 300°K [64]. Figure 3.2 shows the wurzite structure of ZnO. ZnO is a powerful n-type material without deliberately doping. The major source of essential donors comes from the original defects which is oxygen vacancies or zinc interstitials [65].

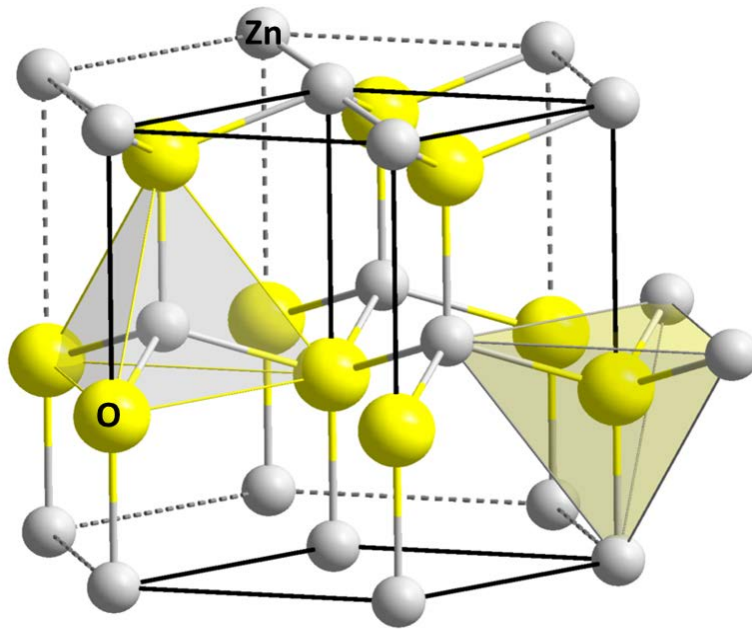


**Figure 3.2. Wurzite structure of ZnO [66]**

### 3.2.2. Properties of ZnO

**Table 3.2. Fundamental properties of ZnO [64]**

Formula weight	81.36g
Density	5.67g/cm <sup>3</sup>
Melting point	2242 K
Lattice constants	a=3.24Å, c=5.2 Å
Thermal expansion coefficient (at 300K)	$\alpha^{\perp}=4.31$ , $\alpha^{\parallel}=2.49$
Dielectric constant	$\epsilon(0)_{\perp c}=7.8$ , $\epsilon(\infty)_{\perp c}=3.7$ , $\epsilon(0)_{\parallel c}=8.75$ , $\epsilon(\infty)_{\parallel c}=3.75$
Hall mobility	$\mu_{\perp c}=70$ , Thin film $\mu_{\parallel c}=170$ , Bulk single crystal $\mu_{\perp c}=150$ (cm <sup>2</sup> /V sec)

### 3.2.3. ZnO in semiconductor history

The first ZnO research was started in 1920. In 1960 piezoelectric properties of ZnO were investigated and later ZnO was used in acoustic wave devices. After that researchers have been investigating ZnO in areas such as optoelectronics, photovoltaic as well as ferromagnetic properties [67]. Moreover, ZnO is a popular semiconductor material in thin film metal oxide semiconductor field effect transistors (MOSFETs). Research has also been done on p- type doping of ZnO, however, the p-type properties of ZnO are transient and only last for six months. [68].

### 3.2.4. Various methods of depositing ZnO

ZnO semiconductor material can be prepared by various methods. The following sub chapter will discuss some of methods including, sputtering, CVD, sol-gel method, pulsed laser deposition and chemical bath deposition. Electrochemical deposition will be discussed in the following chapter.

Sputtering is one of most popular methods used to produce ZnO semiconductors. The quality of electrical conductivity highly depends on the crystal structure, chemical deposition and sputtering modes such as DC and RF. Moreover, the amount of bias voltage is responsible for the surface homogeneousness and the density of the deposited ZnO layer [69].

There are different types of CVD that can be used to deposit ZnO on the substrate. The surface roughness and thickness of the layer rely on the temperature used during the deposition. Although the deposition temperature affects the band gap energy, the exact correlation between temperature and the amount deposited is unknown [70, 71].

Although the sol-gel method is one of the simplest and cost effective methods, the substrate has to be heated at 300°C for 10 minutes every time it is coated with a solution. In some cases, the same procedure needs to be repeated up to 9 times. After that the substrate needs to be heated at 500°C for two hours to achieve compact ZnO deposition [72].

For pulsed laser deposition, a 248nm KrF excimer laser is used and the pulse frequency and duration are 10 Hz and 10 ns respectively. The deposition takes place for two hours in a  $10^{-4}$  Pa vacuum chamber. The limit of the surface roughness of deposited ZnO is typically between 2-9 nm. An increase in the temperature of the chamber reduces the resistivity of the deposited ZnO [73].

In chemical bath deposition, the pretreated substrate is immersed into a pH controlled chemical solvent for 30 s to 90 s. After that the substrate is annealed for half an hour at 300°C to crystallize the ZnO. In this process, maintaining the pH is quite important [74].

### **3.3. Cu<sub>2</sub>O - ZnO Hetero-junction**

Cu<sub>2</sub>O and ZnO make one of the most popular and effective p-n junctions. In order to get a hetero-junction, two different semiconductors with different band gap energy are needed. ZnO possesses a 3.3eV band gap energy which is wider than the 2eV band gap of Cu<sub>2</sub>O (Figure 3.3). The Cu<sub>2</sub>O-ZnO photosensitive hetero-junction has received a great deal of attention due to its theoretical energy conversion efficiency of 18% and its higher light absorption coefficient than other silicon photosensitive devices [75].

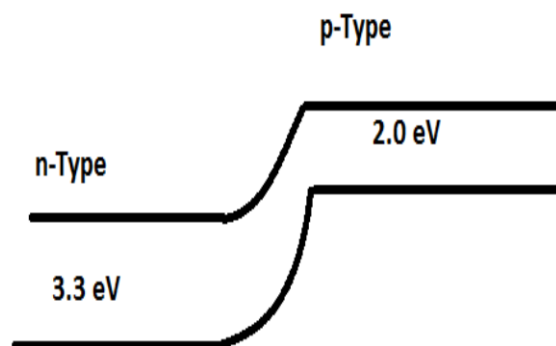


**Figure 3.3. Band-structure of Cu<sub>2</sub>O-ZnO hetero-junction**

Note: Adapted from [76]

There are various existing methods used to produce the Cu<sub>2</sub>O-ZnO junction. However, the two most popular methods are electrochemical deposition and sputtering of both Cu<sub>2</sub>O and ZnO.

### 3.3.1. Efficiency of Cu<sub>2</sub>O-ZnO produced by existing methods

Electrochemical deposition of Cu<sub>2</sub>O for Cu<sub>2</sub>O-ZnO photovoltaic devices can be achieved using three different pH reagents: LiOH, NaOH and KOH. Devices that use LiOH have an energy conversion efficiency of 1.43% while devices that use NaOH and KOH have efficiencies of 0.698 and 0.591% respectively [77]. Low temperature Cu<sub>2</sub>O-ZnO electrodeposited photovoltaic devices have shown to achieve energy conversion efficiencies of 0.1% to maximum 1.28% [78]. Another type of photosensitive device has also been developed by electrodepositing ZnO and Cu<sub>2</sub>O and superimposing this layer with sputtered ZnO. This device provided maximum energy conversion efficiency 1.02%. Whereas a simple electrodeposited layer of ZnO and Cu<sub>2</sub>O only allowed 0.09% of energy conversion efficiency [79]. Another method involves RF sputtering of ZnO followed by electrodeposition of Cu<sub>2</sub>O at different potentials. The energy conversion efficiency of devices developed at a -0.5 V electrodeposition potential was 0.023% and at -0.6 V was 0.24% which was the maximum energy conversion efficiency [80]. Electrodeposition of FTO/ZnO/Cu<sub>2</sub>O resulted in 0.25% energy conversion efficiency

while ITO/ZnO/Cu<sub>2</sub>O and ITO/ZnO/CuO provided  $7.3 \times 10^{-3}\%$  and  $1 \times 10^{-5}\%$  respectively [81].

Although the theoretical energy conversion efficiency of Cu<sub>2</sub>O-ZnO is 18%, in reality, the maximum energy conversion energy obtained for Cu<sub>2</sub>O-ZnO solar cell, using a high temperature annealing and pulse laser deposition technique, is 3.83% [14]. Till date, the maximum efficiency achieved has been far lower than the theoretical efficiency. Therefore, further research is needed to fully understand the material properties of Cu<sub>2</sub>O and thus, boost the maximum energy conversion efficiency.

## **Chapter 4.**

### **Processing technique for paintable photosensitive devices**

Cu<sub>2</sub>O is one of the most attractive semiconductor materials because it is plentiful, low cost and easy to produce. Many researchers have been investigating a simpler alternative to the existing methods of preparation. This thesis presents a unique, cheaper and uncomplicated process technology of producing p-type Cu<sub>2</sub>O on a copper sheet by a painting technique.

The second part of the process involves electrodepositing of ZnO on top of the painted Cu<sub>2</sub>O. Since the Cu-Cu<sub>2</sub>O layer represents a p-type, an n-type semiconductor is required to form a junction. ZnO is one of the most abundant n-type semiconductors and is simple to produce. Cu<sub>2</sub>O and ZnO have been a good match for semiconductor research for decades and has been used in this research. Therefore, the device consists of three layers: copper, Cu<sub>2</sub>O and ZnO. At the end, two electrode connections were made for device characterization.

#### **4.1. Cu<sub>2</sub>O process technology**

##### **4.1.1. Preparation of colloidal suspension paint for Cu<sub>2</sub>O**

The preparation of the colloidal suspension paint consists of three main steps: A mixture adhered hydrate Cu<sub>2</sub>O, de-ionised water and acetone was prepared in a glass container of cuprous chloride. For this, 5 gm of cuprous chloride and adhered hydrate Cu<sub>2</sub>O was added to 10 ml of de-ionised water and stirred thoroughly. 5 ml of acetone was added into the solution and mixed well. Finally, the colloidal suspension was ready for Cu<sub>2</sub>O painting.

#### 4.1.2. Painting process

A bare copper sheet which was made from 99.99% pure copper, of 0.18 mm thickness, 41.1 mm length and 30.4 mm width. First, the copper sheet was cleaned with a very fine sand paper and washed with acetone and de-ionised water thoroughly. The copper sheet was then left to dry. Next, the colloidal suspension paint was applied on the cleaned copper sheet with a small paintbrush evenly and homogenously. Approximately half of the copper sheet was painted and the rest was left to make electrical contact for the device. The paint was allowed to settle for 5 minutes and then it was washed with de-ionised water first and acetone later with the help of a clean cotton swab to remove any contamination of H<sub>2</sub>O. Finally, a clean reddish brown or orange film of homogenous Cu<sub>2</sub>O was formed on the sheet as shown in Figure 7 . After that the device was heated on the hot plate. The device which was heated for 30 minutes at 75 °C was denoted as device (1) and the device which was heated for two hours at 75 °C was denoted as device (2) . After this step both devices were ready for ZnO electrodeposition. Therefore, device (1) and device (2) after ZnO deposition provided different results and the results will be discussed in Chapter 5.



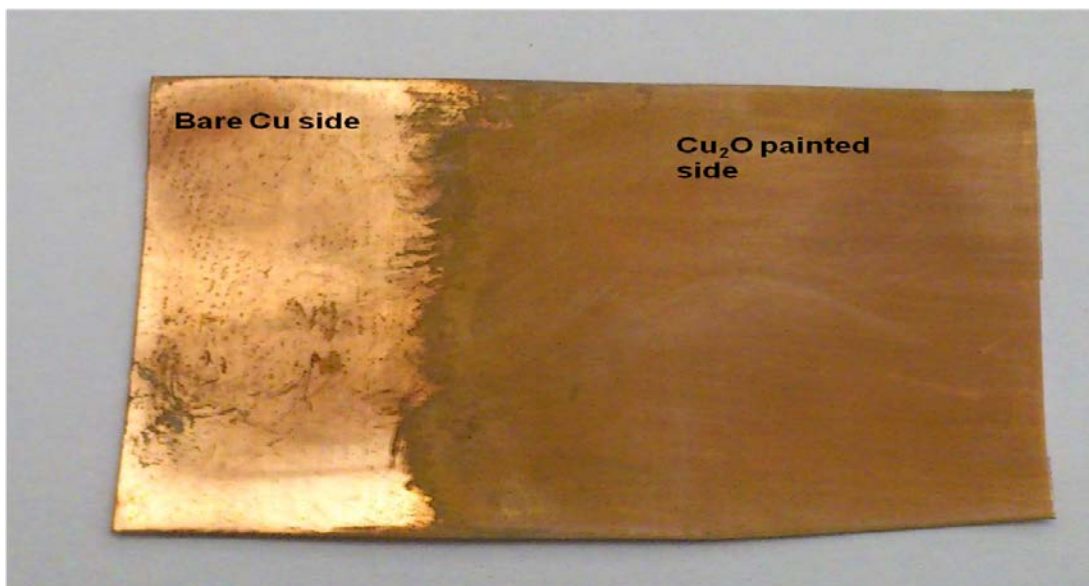


**Figure 4.1. Photograph of the  $\text{Cu}_2\text{O}$  painted on bare Cu sample**

When the painted  $\text{Cu}_2\text{O}$  was heated for longer time than two hours, the longer air exposure time transformed  $\text{Cu}_2\text{O}$  to  $\text{CuO}$ . Therefore, without proper equipment to prevent from air exposure, painted  $\text{Cu}_2\text{O}$  substrate was not able to be heated more than two hours in our experimentation.

## **4.2. ZnO deposition**

There are many approaches to process ZnO such as sputtering, pulsed laser deposition, chemical bath deposition, sol-gel method, chemical vapor deposition and electrochemical deposition. Out of these techniques, electrochemical deposition has the benefits of having control over the area of deposition, being low cost, requiring low process temperatures and being easy to set up.

### **4.2.1. Electrochemical deposition**

Electrochemical deposition has been one of the most popular methods among semiconductor research. Electrochemical deposition provides flexibility and control of variables so that desired product can be achieved. Figure 8 shows the basic electrochemical deposition diagram with the variables that can be controlled during

deposition. In the electrochemical deposition process, the current flow between two electrodes brings the ions from the desired electrode and deposits them on the surface of the other electrode.

There are two types of electrochemical deposition methods: the galvanic method and the potentiostatic method. The galvanic method has been used for electrochemical deposition since the 19th century [82]. The galvanic electrochemical deposition process includes two electrodes and a DC power source connected to those electrodes. The power source is a current source. The two electrodes immersed into the electrolytes are the anode (positive) and the cathode (negative) where oxidation and reduction take place. For the potentiostatic method, three electrodes are required along with a voltage source. These are the anode (positive), cathode (negative) and reference electrodes. The working electrode is an anode when anodic deposition is required.

Working electrode: The required reaction occurs at the working electrode and during electrochemical deposition; the working electrode is usually a substrate with a small surface area. Working electrode should not chemically react with the solution in which it is immersed and the surface of working should not be smooth [83]. In a cathodic deposition, the working electrode is a cathode and the counter electrode is an anode. In an anodic deposition, the working electrode is an anode.

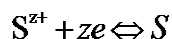
Counter electrode: the counter electrode conveys current to the working electrode through the solution. Using the counter electrode, the electrolyte composition is kept constant during the deposition process [83].

Reference electrode: The reference electrode is only for potential measurement and is not a mandatory for electrochemical deposition. A quality reference electrode shows a constant potential independent of the amount of current during the process. For small amount of current, counter electrode works as reference electrode [83].

#### **4.2.1.1. Electrode potentials during electrochemical deposition**

If a metal named S is immersed into the solution containing metal S ions  $S^{z+}$ , there will be an interchange of  $S^{z+}$  ions between metal S and the solution it is in. The

crystal lattice of metal S will transfer some  $S^{z+}$  ions to the solution and the solution will transfer some ions  $S^{z+}$  to the metal S. One side of the reaction occurs more rapidly than the other side. If more  $S^{z+}$  ions depart from the metal than the reverse direction, there will be an excessive amount of electrons on the surface of the metal. Therefore the metal obtains a negative charge. After a certain period of time, the dynamic equilibrium in the process can be expressed as,



Where, z is the number of electrons participating in the process. From left to right, the reaction accepts electrons and so it is called reduction. On the contrary, in the reserve direction, the reaction releases electrons and so it is called oxidation. During the process, the number of electrons released from the metal is equal to number of electrons accepted by the metal [84].

#### 4.2.1.2. Faraday's Law

Faraday's Law mentions that the weight of the deposited ions at an electrode during electrochemical deposition process is directly proportional to the amount of electricity flowing to that electrode [84]. Mathematically,

$$w = mlt/nF \quad \dots\dots\dots(4)$$

where:

w = weight of the deposited substance

m = molecular weight of the substance

I = current

t=time

$n$  = number electrons transferred

$F$  = Faraday's constant (96,485.309 Coulombs/eqv)

#### 4.2.1.3. Electrochemical deposition of ZnO

Figure 4.2 shows a photograph of the ZnO deposition set-up. It consists of two electrodes, a 250ml beaker and a DC power supply with a 2k-ohm resistor. In this step of the process, device (1) and device (2) were processed in a similar manner.

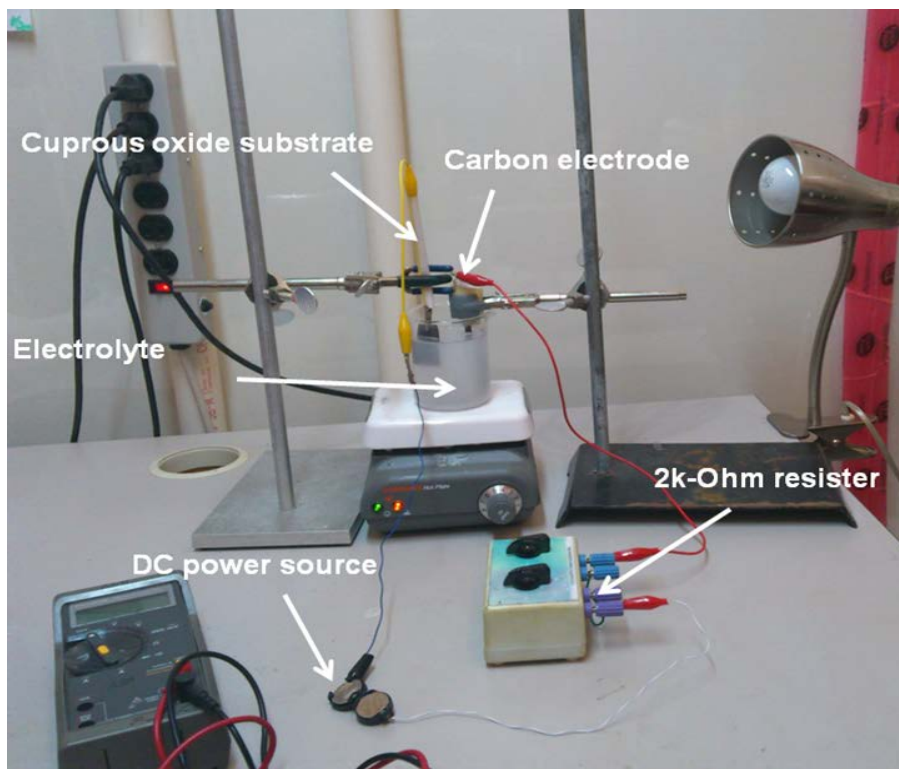


**Figure 4.2. Detail set up of ZnO electrochemical deposition**

Electrodeposition of ZnO was prepared with an ordinary galvanic electrochemical system using two electrodes. The deposition was a cathodic deposition process. The painted  $\text{Cu}_2\text{O}$  was used as the working electrode (cathode) and a carbon electrode was used as counter electrode (anode).

Three two-volt lithium batteries were used as a DC voltage source which was connected with 2 k $\Omega$  resistor to provide a 3mA constant current supply.

0.6g of zinc nitrate was diluted in 250ml of de-ionised water and the resulting pH of the electrolyte solution was 7. In order to reach the desired pH level of 12, NaOH was added into the electrolyte solution. When the desired pH level was reached, the solution was heated on the hot plate and the temperature of the solution was constantly monitored with a thermometer. When the temperature of the solution reached 70°C, the two electrodes were immersed into the solution and connected with a 3mA constant current source which had already been prepared. The deposition was conducted for 4 hours at the maintained temperature of 70°C. At the end of the process, the sample was washed with de-ionised water and dried to prepare for making contact electrodes for the experiment. The ZnO electrochemical deposition can be described as shown in Equations below [85],



During the electrochemical deposition, the reaction rate of equation (5) and (6) increased along with the amount of OH<sup>-</sup> on the surface of the working electrode. Equation (8) shows that the, the extra amount of OH<sup>-</sup> was counterbalanced by attraction of H<sup>+</sup> [81].

#### 4.2.1.4. Results

Using Faraday's law, the weight of the deposited ZnO can be calculated from Equation (4) to be,

$$w=( 81.4084 \times (4 \times 3600) \times 3m) / (2 \times 96485.309) = 0.018225 \text{ grams}$$

In above equation, molecular weight of the ZnO (m) is 81.4084 g/mol. The time (t) was 4 hours, mentioned in seconds in calculation and the current I was 3 mA. The valance electron of ZnO was 2 and Faraday's constant was 96485.309 coulombs/mol. From these variables, the weight of the deposited substance (w) was calculated to be 18.225 mg .

With a known weight and area of the deposited substance, the thickness of the substance could be calculated easily as follows: Volume of the substrate = weight of the substrate / density of ZnO. Therefore, Volume of the substrate = 18.225mg (from calculations above) / 5.506gm/cm<sup>-3</sup>

$$= 3.25 \times 10^{-3} \text{ cm}$$

Thus, the thickness of the substrate = Volume/surface area of the substrate (8)

$$= 3.25 \times 10^{-3} / 4.1174 = 7.89 \text{ } \mu\text{m}$$

### **4.3. Contact electrode**

For testing, two contact electrodes were connected to the prepared device. An insulated wire-wrap wire of approximately 5 cm length was used for these electrical connections. About 1 cm of the sleeve was removed from the wire ends, and the exposed wire tips were attached to the sample by Nickel Conductive Paint 840-20G manufactured by MG-Chemicals. One connection was made to the deposited ZnO layer and the other connection was made to the bare Cu. Figure 4.3 shows the device preparation steps and Figure 4.4 illustrates a completed prototype photosensitive device sample and.

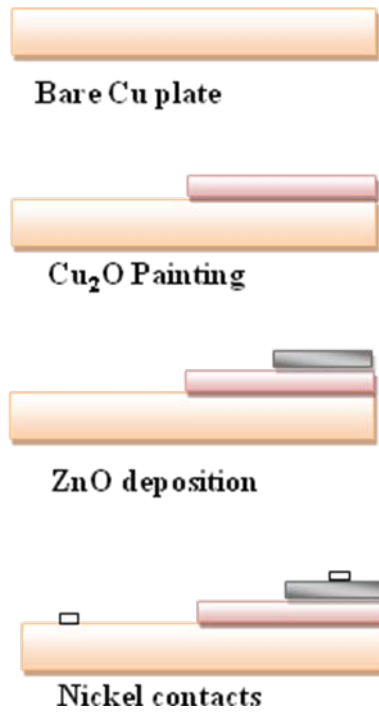


Figure 4.3. Cu- $\text{Cu}_2\text{O}$ -ZnO device processing steps

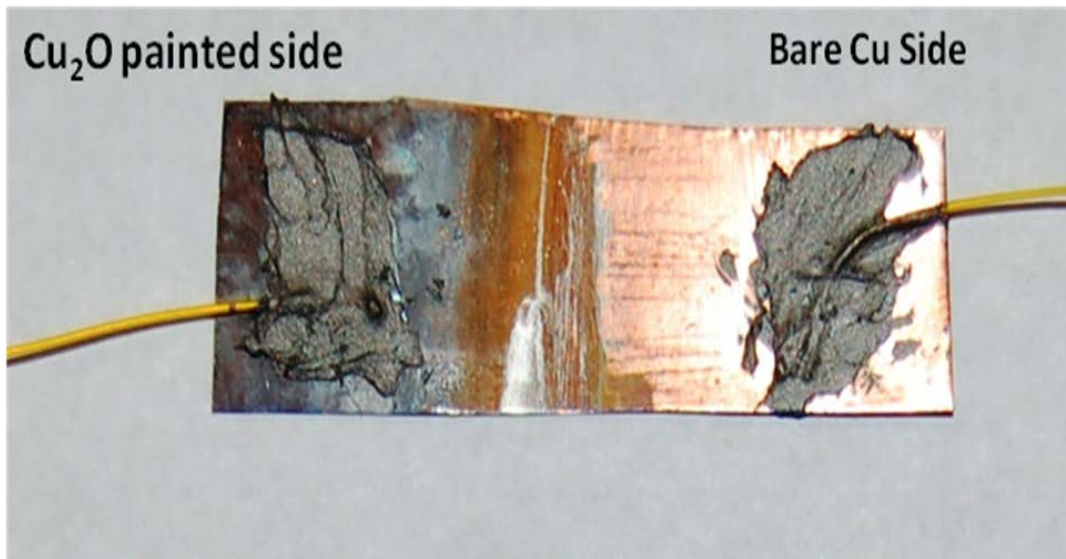


Figure 4.4. A complete Cu- $\text{Cu}_2\text{O}$ -ZnO device with nickel painted electrodes

## 4.4. Surface Morphology

In order to investigate the surface of the device, we used FEI/Aspex Explorer variable pressure SEM (scanning electron microscope) with its oil-free pumping system and W filament. The variable pressure of the vacuum can range between 0.01-1.0 torr for the imaging mode. The range of voltage acceleration is 0.2-25 kV. Although the maximum image resolution of the device is theoretically approximately 20 nm, in reality the image begins to blur beyond 12  $\mu\text{m}$ . The resolution of the electron detectors for FEI/Aspex explorer is 133 eV.

The surface morphology of the painted  $\text{Cu}_2\text{O}$  and deposited ZnO was observed using SEM operating at 20kV. Before ZnO deposition, the surface of the painted  $\text{Cu}_2\text{O}$  substrate was investigated by SEM. The texture of  $\text{Cu}_2\text{O}$  shown in SEM appeared homogenous and this result suggests that painting method of  $\text{Cu}_2\text{O}$  is effective. Figure 4.5(a) shows the painted  $\text{Cu}_2\text{O}$  surface texture. After ZnO deposition, on the surface of the electrodeposited substrate, the ZnO crystals were examined. Figure 4.5 (b) and (c) are the SEM images of ZnO in 12  $\mu\text{m}$  and 20  $\mu\text{m}$  respectively.



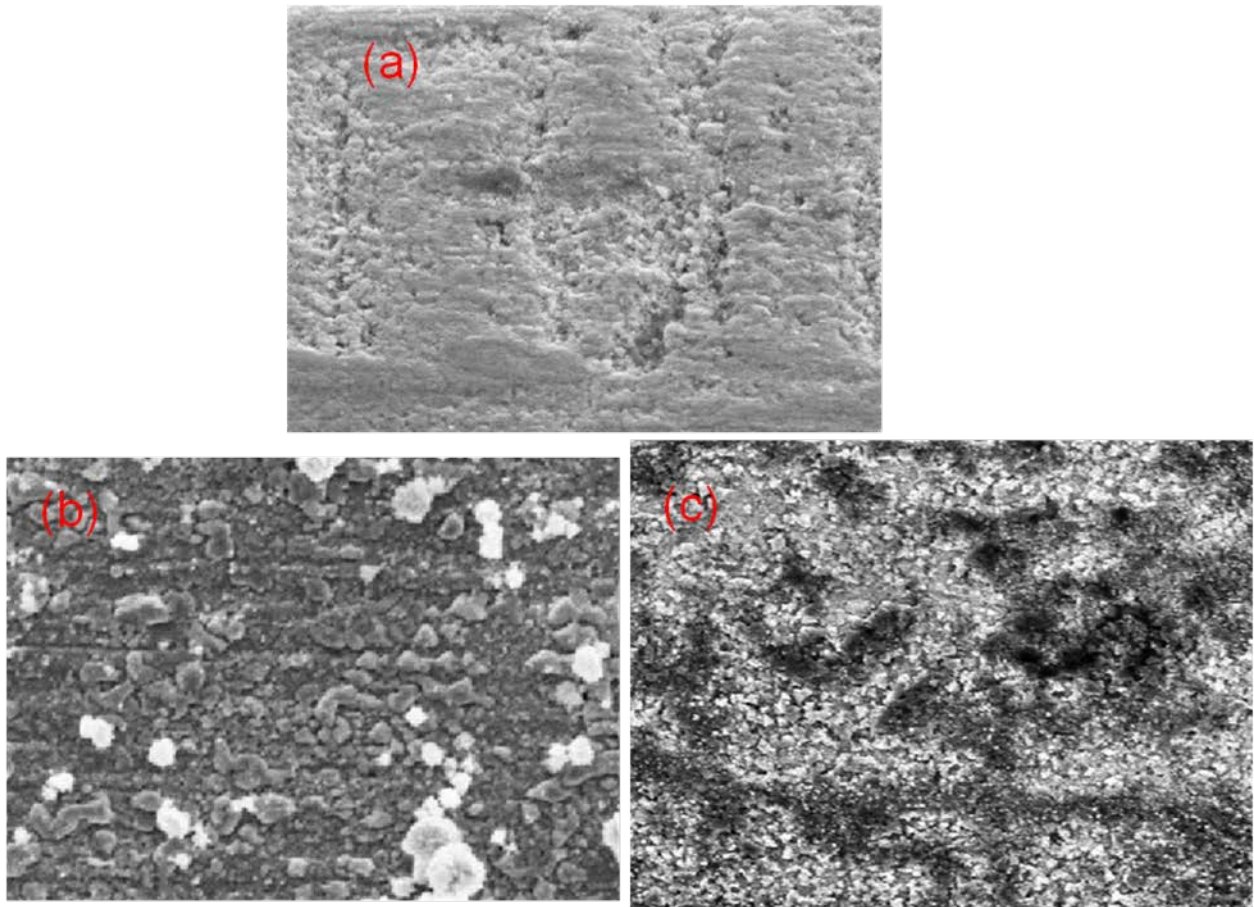


Figure 4.5. (a) SEM image of  $\text{Cu}_2\text{O}$  in  $18\mu\text{m}$ , (b) SEM image of  $\text{ZnO}$  in  $20\mu\text{m}$  and (c) SEM image of  $\text{ZnO}$  in  $12\mu\text{m}$

## 4.5. Electrical Characteristics

The electrical characteristics of cuprous oxide and zinc oxide were investigated by measuring the Hall Effect. The Hall Effect is used to investigate the behavior of charge transport in metal and semiconductor substrates when a combination of a magnetic field and an electric field called Lorentz force is applied to the substrate in a perpendicular direction. Additionally, Hall Effect measurement can be used to distinguish whether the type of semiconductor is n-type or p-type [86].

The magnetic field and the charge  $q$  provide the force on a particle which can be mentioned as the cross product of velocity and magnetic field those are perpendicular to the force vector as shown in equation 9[86].

$$\vec{F} = (q\vec{v}) \times (\vec{B}) \dots\dots\dots(9)$$

Equation 1 shows that the Lorentz force F relies on the charge of the particle q, and the velocity of the particle v due to the presence of an Electric field E and a magnetic field B.

$$\vec{F} = q(\vec{E} + \vec{v} \times \vec{B}) \dots\dots\dots(10)$$

Where,  $\vec{F}$  = Lorentz force,

q= electric charge of particle (1.602x10<sup>-19</sup> C)

$\vec{E}$  = electric field

$\vec{v}$  = velocity of the particle

$\vec{B}$  = magnetic field

When a magnetic field and a constant current source applied are known, Hall voltage can be calculated by using equation 11

$$V_H = \frac{IB}{qnd} \dots\dots\dots(11)$$

Where, I = current

B= magnetic field

d = sample thickness

q= electric charge of a particle

On the other hand, the multiplication of n and d can be mentioned as n<sub>L</sub> (layer density). Therefore,

$$n_L = \frac{IB}{q|V_H|} \dots\dots\dots(12)$$

From the above equation  $n_L$  layer density of charge carriers of a semiconductor can be calculated by using the measured Hall voltage  $V_H$  and given values of I, B and q.

Moreover, Hall mobility can be calculated using the sheet resistance value,

$$\mu = \frac{|V_H|}{R_s IB} \dots\dots\dots(13)$$

Where,  $\mu$  = Hall mobility

$R_s$ =sheet resistance

#### **4.5.1. Hall voltage measurement for Cuprous Oxide**

In order to investigate the semiconductive properties of cuprous oxide, the Hall effect was measured using an instrument which consists of two powerful magnetic coils with variable current supply to adjust the magnetic force acting on the cuprous oxide substrate. Two pairs of electrodes were set up on the surface of the cuprous oxide substrate in order to provide the current supply and measure the Hall voltage ( $V_H$ ). The detailed electrodes setup is shown in figure 4.6.

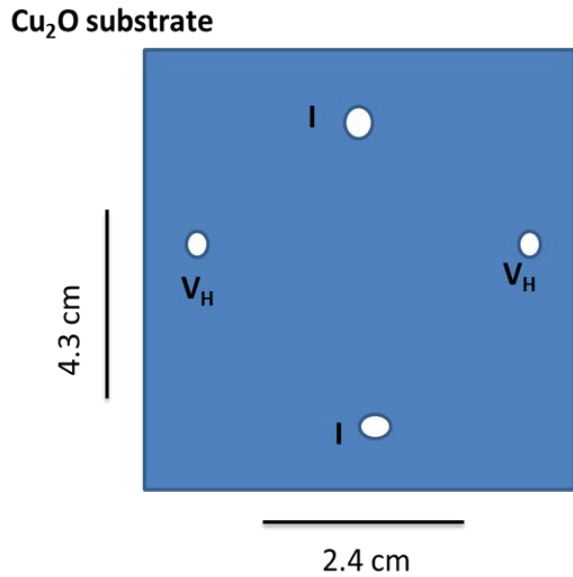


**Figure 4.6. Electrode location details. I – Current electrodes and V – Hall voltage probing electrodes**

The Hall voltage was measured while a supply current of  $53.3 \mu\text{A}$  was being provided under different magnetic field strengths, at room temperature. At first, the current supply was connected between the two electrodes and the multi-meter was connected between the two  $V_H$  electrodes for Hall voltage measurement. After that the magnetic field was applied to the cuprous oxide substrate and the resulting voltage on the multi-meter was recorded. The multi-meter showed a voltage spike, right after the magnetic field was applied. This spike sustained for fraction of a second and then dropped to 0V (steady state). Moreover, there was a very small value of voltage spike approximately 0.2mV after the magnetic field was turned off. In our case, we used the value of the voltage spike after the magnetic field was applied as the Hall voltage and calculated the Hall layer density  $n_L$  and Hall mobility  $\mu$ .

**Table 4.1. Hall Voltage measurement of cuprous oxide**

Magnetic field(Tesla)	Turn on spike (mV)	Turn off spike(mV)	Steady state(mV)	Layer density ( $\times 10^{17} \text{cm}^{-3}$ )	Hall Mobility ( $\text{cm}^2 \text{V}^{-1} \text{sec}^{-1}$ )
0.2	0.29	0.02	0	2.3	13.56
0.4	0.53	0.02	0	2.5	12.38
0.555	0.59	0.06	0	3.17	9.85
0.74	0.99	0.06	0	2.4	12.5
0.875	1.13	0.06	0	2.6	12.07
1	1.26	0.08	0	2.65	11.78

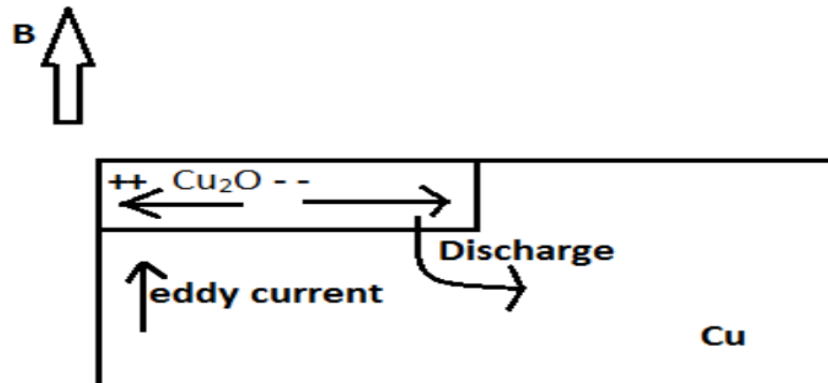


**Figure 4.7. Voltage discharge through copper**

Although there is no previous report of a similar result mentioned, we hypothesize that the voltage spike was due to eddy current ferromagnetic semiconductor cuprous oxide [86]. Furthermore, the conductive and ferromagnetic copper sheet beneath the cuprous oxide layer was causing the cuprous oxide to discharge through the copper sheet. Due to the discharge through the copper sheet, the constant voltage could not be measured before and after the magnetic field was applied. The main purpose of this project was to investigate a simple painting method in order to make cuprous oxide. To do so, the copper sheet had to be underlying a layer of cuprous oxide and the top

most layer of copper sheet was oxidized to a thin layer of cuprous oxide. Therefore, according to nature of the project, it was not possible to make cuprous oxide without the underlying copper sheet which is a conductor and ferromagnetic material. Therefore, according to Hall Voltage measurement, cuprous oxide can be mentioned as a semiconductor although there was a notable abnormality due to voltage discharge through the copper.

#### 4.5.2. Hall voltage measurement for Zinc Oxide

The measurement of Hall voltage for zinc oxide was performed using the same procedure as that used for cuprous oxide. During the Hall Effect measurement for Zinc oxide, the multi-meter for Hall voltage showed a constant voltage of 23 mV. When the magnetic field was applied, the 23mV increased to the certain level depending on the strength of magnetic field for fraction of a second and settled to 23 mV again. The Hall voltage was denoted as the voltage spike just after the magnetic field was applied. We measured the Hall voltage in different magnetic fields and calculated the layer density  $n_L$  and Hall mobility  $\mu$ . Although Eddy currents may have caused the voltage spike, the constant voltage of 23 mV voltage confirmed that the zinc oxide on the glass substrate behaved as a semiconductor.

**Table 4.2. Hall Voltage measurement of zinc oxide**

Magnetic field(Tesla)	Turn on spike (mV)	Turn off spike(mV)	Steady state(mV)	Layer density ( $\times 10^{17} \text{cm}^{-3}$ )	Hall Mobility ( $\text{cm}^2 \text{V}^{-1} \text{sec}^{-1}$ )
0.2	0.52	0.02	0.23	1.28	26.99
0.4	0.76	0.02	0.23	1.76	19.73
0.555	0.94	0.06	0.23	1.99	17.43
0.74	1.17	0.06	0.23	2.1	16.42
0.875	1.42	0.06	0.23	2.06	16.83
1	1.57	0.08	0.23	2.13	16.30

## **Chapter 5.**

### **Photosensitivity of Cu<sub>2</sub>O-ZnO device**

The manufactured device was tested by using an Aligent 4155C Semiconductor Parameter Analyzer (SPA) under the diode characterization settings.

The device was tested for dark current and illuminated current to study its photovoltaic and photo-conductive characteristics. It was also tested under different temperatures to study its temperature dependency. According to the results we have obtained, the device can be characterized under four categories: photo resistivity, photo diode behaviour, photovoltaic behaviour and temperature dependency.

#### **5.1. Experiment and result of Cu<sub>2</sub>O-ZnO device (1) (biased voltage mV)**

The device was tested under diode characterization setting and the voltage sweep was set from -200mV and 200mV. Fiber-Lite high intensity illuminator series 180 manufactured by Dolan-Jenner Industries Inc was used as the illuminating light source. The light intensity was 36.3 mW. Figure 5.1 shows the increase in the current when the device was illuminated. Therefore, the resistance of the device decreased under the illumination of light source.

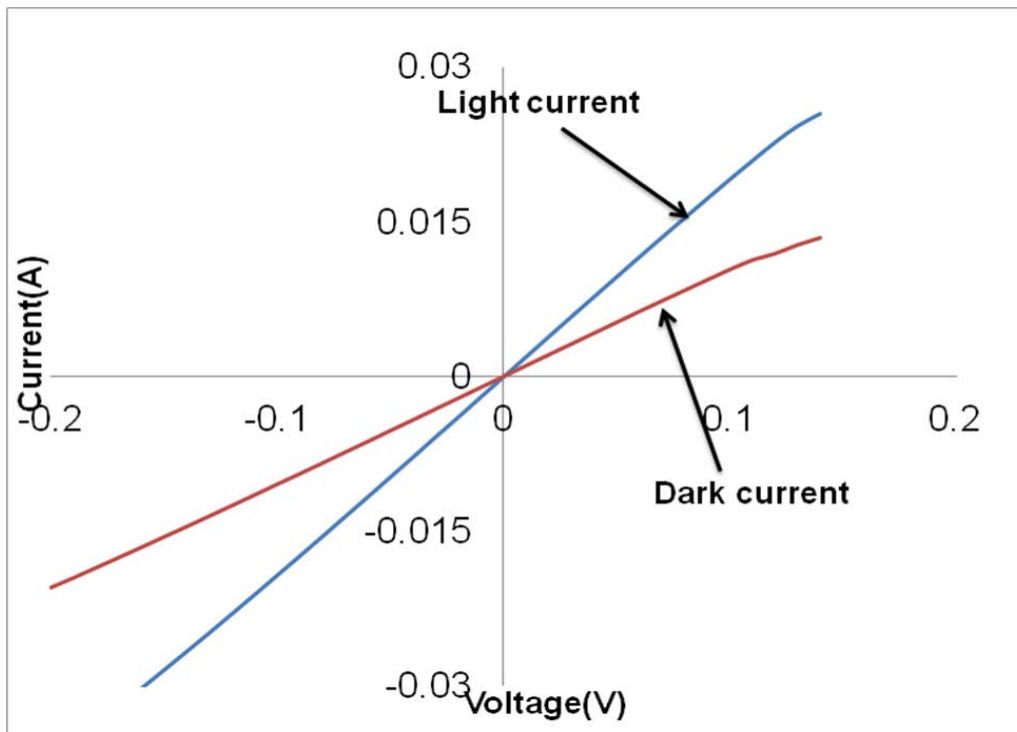


**Figure 5.1. V-I response of the Cu-Cu<sub>2</sub>O-ZnO device (biased voltage mV range)**

According to the V-I response result, the device exhibited more than a 40% increase of current under illumination. On the other hand, the resistance decreased by more than 40% under illuminated current. Therefore, from the characterization result, there was a significant change of resistance when the device was illuminated with a light source. This behavior can be categorized as photo-resistive behavior of the device.

## **5.2. Experiment and result of Cu-Cu<sub>2</sub>O-ZnO device (1) (biased voltage $\mu$ V)**

The same device was tested under the diode characterization setting and the voltage sweep set from -800  $\mu$ V to 800  $\mu$ V. It was tested for dark and illuminated current using the same light source to characterize the V-I characteristics of the device. According to the result, the device behaviour under dark current was ohmic while the behaviour under light current showed diode characteristics.



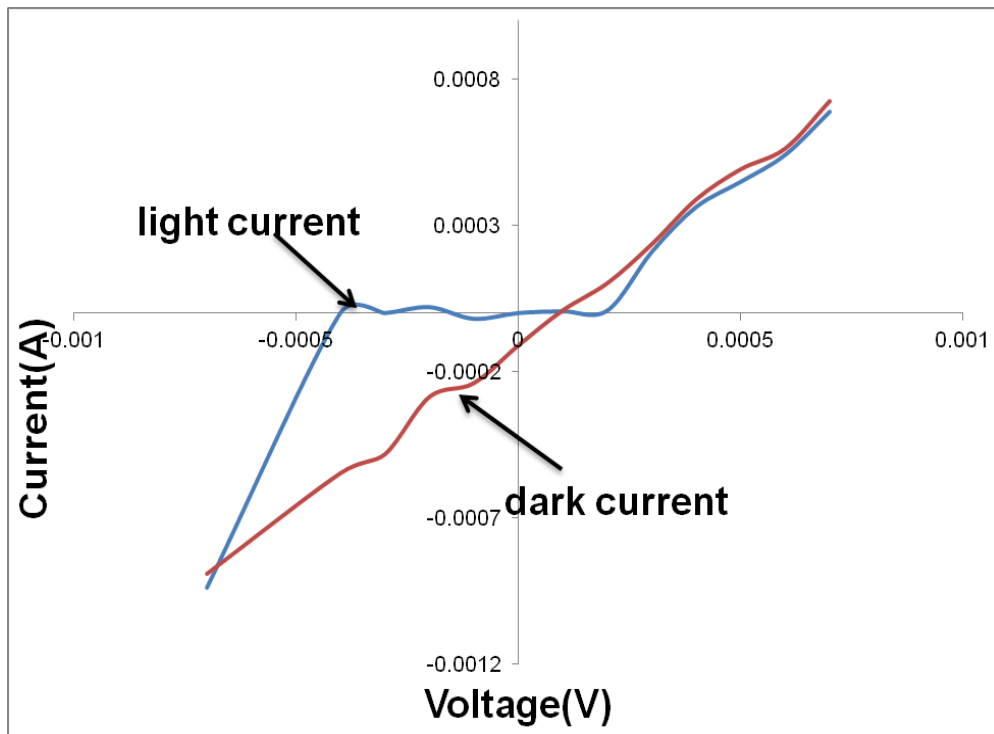
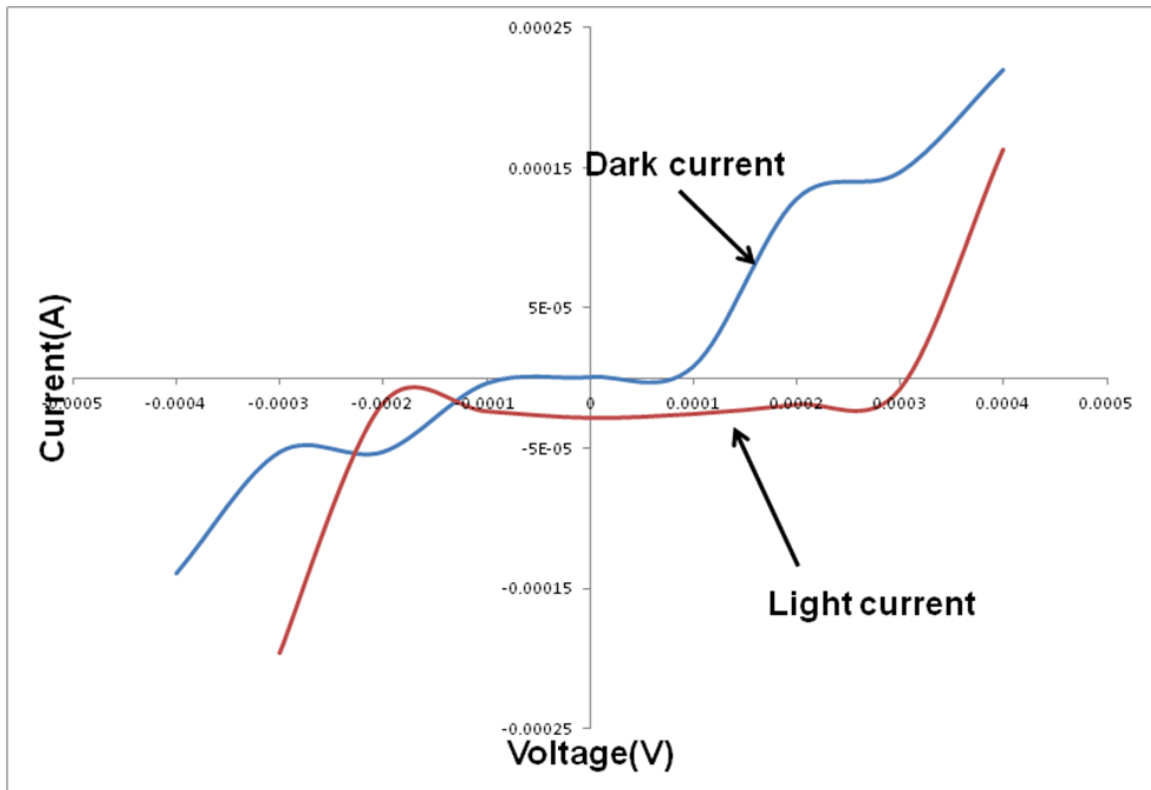


Figure 5.2. V-I response of the Cu-Cu<sub>2</sub>O-ZnO device (biased voltage  $\mu$ V range)

### 5.3. Experiment and results of Cu-Cu<sub>2</sub>O-ZnO Device (2)

Device (2), which was heated for 2 hours after the painting process, did not work at the milli-volt bias range. Therefore it was tested at the micro-volt biased voltage range under dark and illuminated current. The result for this device is shown in Figure 5.3 and behaved as a solar cell. The diode characteristic response under illumination showed the increasing amount of current flow which is a typical behavior of a solar cell.



**Figure 5.3. V-I response of the device observed as a solar cell**

According to the graph, the data values were observed as  $V_{oc} = 0.3 \mu\text{V}$ ,  $I_{sc} = 25 \mu\text{A}$  and Fill factor = 0.32 at the input light power 36.4 mW . From these values, energy conversion efficiency was calculated to be approximately  $6.59 \times 10^{-6}\%$ . The theoretical energy conversion was approximately 0.034% calculated from  $V_{oc} = 0.3 \mu\text{V}$ , fill factor = 0.32 and  $I_{sc} = 0.144 \mu\text{A}$  (calculated by dividing  $V_{oc}$  by device resistance  $2.077 \Omega$ ).

## Chapter 6.

### Conclusion

The goal of this research was to investigate the photosensitivity of Cu<sub>2</sub>O-ZnO devices prepared by using a painting technique followed by a low temperature electrochemical deposition process. The surfaces of Cu<sub>2</sub>O and ZnO that were examined by SEM showed homogeneousness of the surfaces.

The electrical properties of Cu<sub>2</sub>O and ZnO were investigated by Hall Voltage measurement. Although the results from Cu<sub>2</sub>O showed abnormality due to voltage discharge through copper substrate, it can be determined as a semiconductor. The results achieved from ZnO showed semi-conductive behaviour.

Two devices were prepared and heated for the different times. When tested, the device that was heated for 30 minutes showed V-I characteristics similar to a photo-resistor or LDR. When it was exposed to light, it showed approximately 40% of an increase in current flow in the milli-volt range biased voltage. The same device when tested with a micro-volt biased voltage showed a different result. Under dark current, the V-I characteristics showed ohmic behaviour whereas under a light source it showed diode characteristics. These results unequivocally demonstrate the photosensitive behavior of the Cu/Cu<sub>2</sub>O-ZnO device that has been developed in this research. The second device which was heated for 2 hours showed V-I photovoltaic characteristics. Comparing to dark and light diode characteristics, light diode characteristics showed current increased. However, energy conversion efficiency was only  $6.59 \times 10^{-6}\%$ .

Both shorter and longer heating procedures provided a Cu<sub>2</sub>O-ZnO interface with low device resistances of approximately 2  $\Omega$  which is one of the most important requirements for photosensitive device. Thus, the preparation of Cu<sub>2</sub>O using a simple

painting method followed by ZnO electrochemical deposition successfully showed device with photosensitive and photovoltaic properties with very low device resistance

## Chapter 7.

### Future work

There are a number of areas that need to be considered in further stages of this work to improve the photosensitivity and energy conversion efficiency of the device. In order to maintain the physiochemical conditions that help enhance the stability of  $\text{Cu}_2\text{O}$ , the device should be stored in vacuum desiccators. This would help yield high purity  $\text{Cu}_2\text{O}$  that is free of cupric oxide contaminants. One of the issues in the heating process was that the heating needed to be stopped promptly at two hours. This is because when the sample was heated for more than two hours, the air exposure made the sample contaminated with  $\text{CuO}$ . Therefore, an air tight oven should be used to heat the painted  $\text{Cu}_2\text{O}$  sample to avoid contamination from air exposure. Moreover, in order to investigate the composition of  $\text{CuO}$  in the  $\text{Cu}_2\text{O}$  substrate, XPS examination has to be performed and higher quality SEM, TEM and AFS should be used to determine its homogeneity, crystalline nature, cross section and the thickness. The device purity, thickness and crystalline nature could then be used to determine the diffusion length for the recombination of electrons and holes. This is an important property for improving energy conversation efficiency. Furthermore, prior to the electrochemical deposition of  $\text{ZnO}$  on the  $\text{Cu}_2\text{O}$  surface, bulk resistance should be characterized. In addition, a constant current density should be monitored with a power supply source during  $\text{ZnO}$  deposition. The electrical contacts for electrochemical deposition and V-I measurements should also be improved.

## References

1. Gozar, G. Logvenov, L. F. Kourkoutis, A. T. Bollinger, L. A. Giannuzzi, D. A. Muller and I. Bozovic, "High-temperature interface superconductivity between metallic and insulating copper oxides" *Nature*. Vol 455, October (2008).
2. V. Wood, M. J. Panzer, J. E. Halpert, J. M. Caruge, M. G. Bawendi and V. Bulovic, "Selection of metal oxide Charge Transport layers for colloidal quantum dot LEDs", *American Chemical Society* Vol. 3, p3581-3586 (2009).
3. P. He, X. Shen, H. Gao, "Size-controlled preparation of Cu<sub>2</sub>O octahedron nanocrystals and studies on their optical absorption", *Journal of Colloid and Interface Science*, vol 284, pp 510- 515, (2005).
4. P. A. Korzhavyi, B. Johansson, "Literature review on the properties of cuprous oxide Cu<sub>2</sub>O and process of copper oxidation", October 2011, [Online], Available: <http://skb.se/upload/publications/pdf/TR-11-08.pdf>.
5. D. A. Neamen, "Semiconductor Physics and Devices Basic Principles", McGraw-Hill, (2003).
6. K. Fujimoto, T. Oku, T. Akiyama and A. Suzuki, "Fabrication and characterization of copper oxide-zinc oxide solar cells prepared by electrodeposition", *Journal of Physics:Conference series* 433(2013).
7. J. Kayama, K. Ito, M. Matsuoka and J. Tamaki, "Performance of Cu<sub>2</sub>O/ZnO solar cell prepared by two-step electrodeposition", *Journal of Applied Electrochemistry* 34, p687-692, (2004).
8. S. S. Jeong, A. Mittiga, E. Salza, A. Masci and S. Passerini, "Electrodeposited ZnO/Cu<sub>2</sub>O hetero-junction solar cells", *Electrochimica Acta* 53, p 2226-2231(2008).
9. S. Hussian, C. Cha, G. Nabi, W. S. Khan, Z. Usman and T. Mahmood, "Effect of electrodeposition and annealing of ZnO on optical and photovoltaic properties of the p-Cu<sub>2</sub>O-n-ZnO solar cells", *Electrochimica Acta* vol56, p 8342-8346, (2011).
10. A. S. Zoolfakar, R. A. Rani, A. J. Morfa, S. Balendran, A. P. O'Mullane, S. Zhuiykov and K. Kalantar-zadeh, "Enhancing the current density of electrodeposited ZnO-Cu<sub>2</sub>O solar cells by engineering their heterointerfaces" *J. Mater. Chem.*, vol22, (2012).

11. P. A. Kotsyumakha and N. P. Likhobabin "Cuprous Oxide Photoresistors" UDC 621.38.
12. T. Zhai, X. Fang, M. Liao, X. Xu, H. Zeng, B. Yoshio and D. Golberg, "A Comprehensive Review of one-dimensional Metal-Oxide Nanostructure Photodetectors" *Sensors*, vol 9, p6504-6529, (2009).
13. C. C. Chao, Y. Ohkura, T. Usui and J. M. Weisse, "Methods for Improving Efficiencies of Cuprous Oxide Solar Cells", [Online]. Available: <http://web.stanford.edu/~ccchao1/Solar%20Cells/MATSCI%20302%20Cu2O%20Solar%20Cells.pdf>.
14. T. Minami, Y. Nishi, T. Miyata and J. Nomoto, "High-Efficiency oxide solar cells with ZnO/Cu<sub>2</sub>O hetero-junction Fabricated on thermally oxidized Cu<sub>2</sub>O sheets", *Applied Physics Express* vol 4, (2011).
15. Photo-resistor: [Online] Available: <http://www.resistorguide.com/photoresistor/>.
16. Diode, LDRs and Thermistors: [Online] Available: <http://www.passmyexams.co.uk/GCSE/physics/diodes-LDR-thermistors.html>
17. B. Koren, "Photodiode", *spie's oe magazine*, p 34-36 August (2001).
18. H. T. Hsueh, S. J. Chang, W. Y. Weng, C. L. Hsu, T. J. Hsueh, F. Y. Hung, S. L. Wu and B. T. Dai, "Fabrication and Characterization of Coaxial p-Copper oxide/n-ZnO Nanowire photodiodes", vol 11, p 127-133, Jan (2012).
19. Photodiode light detector [Online] Available: <http://hyperphysics.phy-astr.gsu.edu/hbase/electronic/photdet.html>.
20. H. Hoppe and N. S. Sariciftci "Organic solar cells: An overview", *J. Mater. Res.*, vol 19, p 1924-1945 (2004).
21. S. Ruhle, A. Y. Anderson, H. Barad, B. Kupfer, Y. Bouhadana, E. Rosh-Hodesh and A. Zaban, "All-oxide photovoltaics", *The journal of physical chemistry letters*, vol 3, p3755-3764 (2012).
22. Basic Si solar cell [Online] Available: [http://www.tf.uni-kiel.de/matwis/amat/semitech\\_en/kap\\_8/backbone/r8\\_1\\_2.html](http://www.tf.uni-kiel.de/matwis/amat/semitech_en/kap_8/backbone/r8_1_2.html).
23. M. Jorgensen, K. Norrman, F. C. Krebs, "Stability/ degradation of polymer solar cell", *Solar Energy Materials & solar Cells* vol 92, p 686-714 (2008).
24. J. Y. Kwon, D. J. Lee and K. B. Kim, "Review Paper: Transparent Amorphous Oxide Semiconductor Thin Film Transistor", *Electronic Materials Letters*, vol 7, p 1-11, No. 1(2011).

25. S. Kose, F. Atay, V. Bilgin and I. Akyuz, "Some physical properties of CdO thin films used as window Material in photovoltaic solar cells", *International Journal of Green energy*, vol 2, p353-364, (2004).
26. Q. Yang, Y. Wu, Y. Liu, C. Pan and Z. L. Wang, "Features of the pie-phototronic effect on optoelectronic devices based on wurtzite semiconductor nanowires", *Phys. Chem. Chem. Phys.*, vol16,p2790-2800, (2014).
27. P. A. Kotsyumakha and N. P. Likhobabin, "Cuprous oxide photoresistors", Chernovtsy State University. Translated from *Izvestiya VUZ. Frzika*, vol. 11, p 137-139 (1968).
28. P. K. Nair, O. G. Daza, A. A. C. Readigos, J. Campus and M. T. S. Nair, "Formation of conductive CdO layer on CdS thin films during air heating", *Semicond. Sci. Technol.* vol 16, p 651-656, (2001).
29. A. Tadjarodi, M. Imani and H. Kerdari, "Application of a facile solid-state process to synthesize the CdO spherical nanoparticles" *International Nano Letters*, vol 3, (2013).
30. J. K. Dunnick, "NTP Technical report on Toxicity studies of cadmium oxide", March 1995 [Online]: Available : [http://ntp.niehs.nih.gov/ntp/htdocs/st\\_rpts/tox039.pdf](http://ntp.niehs.nih.gov/ntp/htdocs/st_rpts/tox039.pdf).
31. H. Yang, Q. Tao, X. Zhang, A. Tang, J. Ouyang, "Solid-state synthesis and electrochemical property of SnO<sub>2</sub>/NiO nanomaterials", *Journal of Alloys and Compounds*, vol 459, p 98-102 (2008).
32. M. N. Rifaya, T. Theivasanthi and M. Alager "Chemical Capping Synthesis of Nickel Oxide Nanaoparticles and Their Charactrizations Studies", *Nanoscience and Nanotechnology*, vol 2(5), p 134-138, (2012).
33. J. Jung, D. L. Kim, S. H. Oh and H. J. Kim, "Stability enchancement of organic solar cells with solution-processed nickle oxide thin films as hole transport layers", *Solar energy Materials & Solar cell* vol 102, p 103-108 (2012).
34. J. Luo, S. K. Karuturi, L. Liu, L. T. Su, A. L. Y. Tok and H. J. F, "Homogeneous photosensitization of comple TiO<sub>2</sub> Nanostructures for efficient solar energy conversion" *Scientific reports*, June (2012).
35. A. N. Banerjee, "The design, fabrication and photocatalytic utility of nanostructured semiconductors: focus on TiO<sub>2</sub>-based nanostrustures" *Nanotechnology, Science and Applications* vol 4, p 35-65, (2011).
36. J. Nowotny, "Oxide semiconductors for solar energy conversion: Titanium dioxide", Chapter 8, p323-381
37. W. Y. Ching, Young-Nian Xu and K. W. Wong, "Ground-state and optical properties of Cu<sub>2</sub>O and CuO crystals". *Physical Review B*, vol. 40, pp. 7684-7695, Oct (1989).



38. H. Raebiger, S. Lany and A. Zunger, "Origins of the p-type nature and cation deficiency in Cu<sub>2</sub>O and related materials", *Physics Review B*, 76, 045209, July (2007).
39. B. K. Meyer, A. Polity, D. Reppin, M. Becker, P. Hering, B. Kramm, P. J. Klar, T. Sander, C. Reindl, C. Heiliger, M. Heinemann, C. Muller, C. Ronning, "The Physics of cuprous oxide", *Semiconductors and Semimetals*, vol 8, p 201-222, Elsevier Inc., (2013).
40. Copper(I)oxide [online]: Available [http://en.wikipedia.org/wiki/Copper%28I%29\\_oxide#mediaviewer/File:Copper%28I%29-oxide-unit-cell-A-3D-balls.png](http://en.wikipedia.org/wiki/Copper%28I%29_oxide#mediaviewer/File:Copper%28I%29-oxide-unit-cell-A-3D-balls.png)
41. L. O. Grondahl, "Unidirectional current carrying device", Aug 23, 1937
42. W. H. Brattain, "The copper oxide rectifier", *Review of Modern Physics*, vol. 23, July (1951).
43. Charles Fritts, [Online], Available: [http://en.wikipedia.org/wiki/Charles\\_Fritts](http://en.wikipedia.org/wiki/Charles_Fritts)
44. Physics history, [Online], Available: <http://www.aps.org/publications/apsnews/200904/physicshistory.cfm>
45. Aleksandr Stoletov and first solar cell [Online], Available: <http://www.ecotuesday.com/blog/2010-08/daily-cleantech-aleksandr-stoletov-and-first-solar-cell>
46. L. O. Grondahl, "The copper-cuprous oxide rectifier and photoelectric cell", *Review of modern physics*, vol 5 p141-168, April (1933).
47. E. D. Wilson, May 1935, [Online] Available <http://www.google.com/patents/US2095782>
48. D. M. Chaplin, C. S. Fuller and G. L. Pearson, "A New silicon p-n junction photocell for converting solar radiation into electrical power", *J. Appl. Phys.* vol 25, p 676, (1954).
49. L. C. Olsen, F. W. Addis and W. Miller "Experimental and theoretical studies of Cu<sub>2</sub>O solar cell", *Solar cells*, vol 7, p 247-279, (1982-1983).
50. L. C. Olsen, R. C. Bohara and M. W. Urie, "Explanation for low efficiency Cu<sub>2</sub>O Schottkybarrier solar cells", *Applied Physics Letters*, vol 34, p 47-49, (1979).
51. A. E. Rakhshani, "Preparation, Characteristics and photovoltaic properties of cuprous oxide-a review", *Solid-state electronics*, vol 29, p 7-17, (1986).

52. K. V. Rajani, S. Daniels, E. McGlynn, R. P. Gandhiraman, R. Groarke and P. J. McNally, "Low temperature growth technique for nanocrystalline cuprous oxide thin films using microwave plasma oxidation of copper", *Materials letters*, vol 71, p160-163, (2012).
53. J. B. Liang, N. Kishi, T. Soga, T. Jimbo and M. Ahmed. "Thin cuprous oxide films prepared by thermal oxidation of copper foils with water vapor". *Thin solid films* 520, p. 2679-2682. (2012).
54. P. E. De Jongh, D. Vanmaekelbergh and J. J. Kelly. "Photoelectrochemistry of Electrodeposited  $\text{Cu}_2\text{O}$ ", *Journal of The Electrochemical Society*, 147(2), P 486-489 (2000).
55. K. Han, M. Tao. "Electrochemically deposited p-n homojunction cuprous oxide solar cells", *Solar Energy Materials & Solar Cells*, 93, p 153-157 (2009).
56. T. Maruyama. "Copper Oxide Thin Films prepared from copper dipivalomethanate and oxygen by Chemical Vapor Deposition", *Jpn. J. Appl. Phys.* vol. 37, p 4099-4102, (1998).
57. G. Guglietta, T. Wanga, R. Pati, S. Ehrman and R. A. Adomaitis, "Chemical vapor deposition of copper oxide films for photoelectrochemical hydrogen production", *Proc of SPIE*, Vol. 7408, 740807-1(2009).
58. A. Parretta, M. K. Jayaraj, A. D. Nocera, S. Loreti, L. Quercia, and A. Agati, "Electrical and Optical Properties of Copper oxide Films prepared by Reactive RF Magnetron Sputtering", *phys. stat. sol. (a)* 155, 399 (1996).
59. A. A. Ogwu, T. H. Darma, E. Bouquerel, "Electrical resistivity of copper oxide thin films prepared by reactive magnetron sputtering", *Journal of Achievements in Materials and Manufacturing Engineering*, vol 24, p 172-177, September (2007).
60. M. Seo, T. Iwata and N. Sato, "Composition and Structure of Anodic Oxide Films on Copper in neutral and weakly alkaline Borate solutions", *Bulletin of the Faculty of Engineering, Hokkaido University* No 102(1981).
61. E. S. Ikata and S. K. Adjepong, "Electrical characteristics of Cu-Cu<sub>2</sub>O diodes fabricated by anodic oxidation" *J. Phys. D:Appl. Phys*, vol 21, p 1516-1518 (1988).
62. S. Bugarinovic, M. Rajcic-Vujasinovic, Z. Stevic and V. Grekulovic. "Cuprous Oxide as an Active Material for solar cells"<http://cdn.intechopen.com/pdfs-wm/23401.pdf>.
63. M. T. S. Nair, L. Guerrero, O. L. Arenas, P. K. Nair, "Chemically deposited copper oxide thin films: structural, optical and electrical characteristics", *Applied Surface Science* vol. 150. p 143-151(1999).

64. K. Ellmer, A. Klein and B. Rech, "Transparent Conductive Zinc Oxide", Springer.,2007, [Online], Available: <http://link.springer.com/book/10.1007%2F978-3-540-73612-7>.
65. D. C. Look and J. W. Hemsky, "Residual Native Shallow Donor in ZnO", Physical Review Letters, Vol 82, March (1999).
66. Zinc oxide [online] ,Available :  
[https://en.wikipedia.org/wiki/Zinc\\_oxide#/media/File:Wurtzite\\_polyhedra.png](https://en.wikipedia.org/wiki/Zinc_oxide#/media/File:Wurtzite_polyhedra.png)
67. A. Onodera and M. Takesada"Electronic Ferroelectricity in II-VI Semiconductor ZnO"[Online], Available: <http://www.intechopen.com/books/advances-in-ferroelectrics/electronic-ferroelectricity-in-ii-vi-semiconductor-zno>.
68. B. Q. Cao,MLorenz, G. Zimmermann, C. Czekalla, M. Brandt, H. Wenckstern, and M. Grundmann, "p-Type Phosphorus Doped ZnO Wires for Optoelectronic Application",[Online], Available: <http://cdn.intechopen.com/pdfs-wm/10507.pdf>.
69. W. Gao and Z. Li, "ZnO thin films produced by magnetron sputtering", Caramics International, vol 30 p 1155-1159, (2004).
70. T. M. Barnes, J. Leaf, C. Fry and C. A. Wolden, "Room Temperature chemical vapor deposition of c-axis ZnO", Journal of Crystal Growth, vol 274, p412-417, (2005).
71. S. Nicolay, M. Benkharia, L. Ding, J. Escarre, G. Bugnon, F. Meillaud and C. Ballif, "Control of CVD-deposited ZnO films properties through water/DEZ ratio:Decoupling of electrode morphology and electrical characteristics", Solar Energy Materials & Solar Cells, vol105, p46-52 (2012).
72. L. Znaidi, T. Touam, D. Vrel, N. Souded, S. B. Yahia, O. Brinza, A. Fischer and A. Boudrioua, "ZnO Thin Films Synthesized by Sol-Gel Process for Phoronic Applications", Acta Physica Polonica A,vol. 121 (2012).
73. M. G. Tsoutsouva, C. N. Panagopoulos, D. Papadimitriou, I. Fasaki, and M. Kompitsas"ZnO thin films prepared by pulsed laser deposition", Materials Science and Engineering B, vol 176, p 480-483 (2011).
74. Y. Lare, A. Godoy, L. Cattin, K. Jondo, T. Abachi, F. R. Diaz, M. Morsli, K. Napo, M. A. del Valle and J. C. Brenede, "ZnO thin films fabricated by chemical bath deposition used as buffer layer in solar cells", Applied Surface Science,vol 255, p 6615-6619, (2009).
75. B. M. Fariza, J. Sasano, T. Shinagawa,H. Nakano, S. Watase and M. Izaki, "Electrochemical growth of (0001)-nZnO film and the characterization of the hetero-junction diode", J. Electrochem. Soc, vol 158 (2011).

76. D. DeMeo, S. MacNaughton, S. Sonkusale and T. E. Vandervelde, "Electrodeposited Copper oxide and Zinc Oxide core-shell Nanowire photovoltaic cells"[Online], Available: <http://cdn.intechopen.com/pdfs-wm/16350.pdf>.
77. K. Fujimoto, T. Oku and T. Akiyama, "Fabrication and Characterization of ZnO/Cu<sub>2</sub>O solar cells prepared by electrodeposition", Applied physics express, vol 6, p086503-1, (2013).
78. M. Izaki, T. Shinagawa, K. Mizuno, Y. Ida, M. Inaba and A. Tasaka, "Electrochemically constructed p-Cu<sub>2</sub>O/n-ZnO hetero-junction diode for photovoltaic device", J. Phys. D: Appl. Phys, vol 40, (2007).
79. A. S. Zoolfakar, R. A. Rani, A. J. Morfa, S. Balendhran, A. P. O'Mullane, S. Zhuiykov and K. Kalantar-zadeh, "Enhancing the current density of electrodeposited ZnO-Cu<sub>2</sub>O solar cells by engineering their heterointerfaces", J. Mater. Chem, vol 22, p-21767-21775, (2012).
80. S. Hussian, C. Cao, G. Nabi, W. S. Khan, Z. Usman, T. Mahmood, "Effect of electrodeposition and annealing of ZnO on optical and photovoltaic properties of the p-Cu<sub>2</sub>O/n-ZnO solar cell", Electrochimica Acta vol 56, p-8342-8346, (2011).
81. K. Fujimoto, T. Oku, T. Akiyama and A. Suzuki, "Fabrication and characterization of copper oxide-zinc oxide solar cells prepared by electrodeposition", vol 433, (2013).
82. E. M. Garcia, V. F. C. Lins and T. Matencio, "Metallic and Oxide Electrodeposition"[Online], Available: <http://cdn.intechopen.com/pdfs-wm/44716.pdf>.
83. D. Pletcher, R. Greff, R. Peat, L. M. Peter and J. Robinson, "Instrumental Methods in Electrochemistry", Southampton Electrochemistry Group, (1985).
84. M. Paunovic, M. Schlesinger and D. D Snyder "Modern electroplating", John Wiley & Sons., p 1-32, (2010) .
85. M. Izaki and T. Omi, "Electrolyte Optimization for Cathodic Growth of Zinc Oxide Films", vol 143, L53-L55, March (1996).
86. E.M. Purcell and D.J. Morin, "Electricity and Magnetism" Cambridge University Press, 3<sup>rd</sup> edition (2013).